isozymes [14]. Paclitaxel was also metabolized by cytochrome P450 enzymes of the CYP3A and CYP2C subfamilies in hepatic metabolism [13]. The coadministration of these agents with a common metabolic pathway may appear to influence drug concentration and increase adverse effects. Some p-glycoprotein inhibitors have been shown to modulate the pharmacokinetic parameters of chemotherapeutic agents in pre-clinical and clinical studies, and these inhibitors often enhanced toxicity as evidenced by an increase in the AUC of anti-cancer agents. However, concerning drug resistance, the concurrent use of chemotherapeutic and endocrine agents may be reasonable.

Weekly paclitaxel therapy was well-tolerated, with favorable safety and efficacy [27]. In previously published reports on weekly paclitaxel treatment (80–100 mg/m^2 per week) [28, 29], the toxicity was mild and consisted mainly of neutropenia and neuropathy. Severe adverse events included 14–18% grade 3–4 neutropenia, and 4–24% severe neuropathy. Myalgia and arthralgia were common but rarely severe. Toremifene has been also considered to be a promising agent with no serious side effects for use in breast cancer treatment [30, 31]. In phase III trials of standard or high-dose regimen comparisons, adverse events in patients who received 60-mg/day standard doses occurred in less than 20% of the patients [32], and frequent adverse events included hot flashes, sweating, nausea and/or vomiting, vaginal discharge, dizziness, edema, vaginal bleeding, liver function abnormalities, ocular changes and thromboembolic or cardiac events [32–34]. With high doses of toremifene (200 or 240 mg) in phase III studies, there was a trend toward more nausea, reversible corneal keratopathy, clinically insignificant serum glutamic oxaloacetic transaminase elevations, and hypercalcemia compared with tamoxifen [33, 34]. Toremifene appeared equally tolerated at high (up to 240 mg) and low (60 mg) dosage with the exception of a significantly higher incidence of nausea at high dosage in one study [19, 35]. In Japan, high-dose toremifene at 120 mg/day is approved for the treatment of patients refractory to tamoxifen or other agents. In a phase II study by Asaishi *et al*, adverse events occurred in 5.1% of patients and included nausea, vertigo, and abnormal liver function [36]. It is noted that in our study compared with other studies, most patients were treated heavily with prior chemotherapy. They had already complained of various symptoms or had abnormal laboratory data reflecting side effects. Although this study was conducted over a relatively short period, all patients tolerated the treatment well. Only 1 patient (6.7%) had grade 3 neutropenia and for this patient, the administration of paclitaxel was often postponed until neutropenia improved and the treatment was continued with prophylaxis G-CSF. In the follow-up study, 1 patient complained of grade 3 sensory neuropathy and declined to continue the therapy. No other patients experienced severe adverse events and continued to receive the therapy until tumor progression. Actually, some studies showed an increase in hematological toxicities by the addition of a p-glycoprotein modulator [25]. In our study, pharamacokinetics interactions between toremifene and paclitaxel were under the investigation, but the dose reduction may be needed, depending on the analysis.

The benefits of chemoendocrine therapy compared to hormonal therapy or chemotherapy remains unclear. As for the adjuvant chemoendocrine therapy, a study of the SWOG 8814 trial showed that the sequential use of tamoxifen with cyclophosphamide, doxorubicin, and 5-fluorouracil in postmenopausal women with hormone receptor-positive, node-positive breast cancer resulted in better disease-free survival compared to their concurrent use [37]. In advanced or metastatic breast cancer, combining hormonal therapy with chemotherapy was considered to have a potential benefit through additive or synergistic cytotoxicity in hormone receptor-positive breast cancer [38]. But previous studies show no survival advantage for the addition of hormonal therapy to chemotherapy compared to sequential therapy [38]. In our study, because most patients receiving previous various therapies acquired multidrug resistance, chemosensitizing activity rather than additive or synergistic cytotoxicity would be expected.

Paclitaxel is an effective agent in the treatment of metastatic breast cancer and administration schedules of weekly paclitaxel by 1-hour infusion at doses ranging from 80 to 100 mg/m^3 has achieved overall response rates of 50–68% [39]. In pretreated patients with metastatic breast cancer, response rates were in the range of 22–53% with a median time to progression of 5–6 months [29]. On the other hand, in a large phase III study of toremifene therapy for advanced breast cancer, response rates in the high-

dose toremifene arms were 22.6% in the North American Trial [35] and 28.7% in the Eastern European Trial [40], with a median time to progression from 5.5 to 6.1 months. Furthermore, high-dose toremifene therapy (120 to 240 mg/day) in a phase II study in patients with advanced breast cancer refractory to tamoxifen therapy achieved a 0 to 14% objective response rate, and a 19 to 44% disease stabilization during toremifene treatment with a median duration of disease stabilization of more than 2 months [19]. In a Japanese phase II study, Asaishi *et al.* reported that 120 mg of toremifene daily achieved an objective response rate of 14% and disease stabilization of 19% in patients with tamoxifen-refractory breast cancer [19, 36]. In our study, most of the patients had already been exposed and become refractory to various chemotherapeutic or endocrine agents. Notably, our study included 11 (73%) patients exposed to taxanes. In this disadvantageous state, objective response and disease stabilization were observed in 1 (6.7%) and 4 (26.7%) patients, respectively. Overcoming drug resistance is highly suspected beyond our expectations.

In conclusion, the results of this study demonstrate the tolerability and effectiveness of paclitaxel combined with toremifene in patients with metastatic breast cancer. Only 1 patient partially responded in terms of the suspected release of drug resistance. This result is promising in patients previously exposed to multi-drug therapy. In addition in deteriorated patients, this therapy is safe and tolerant as salvage chemotherapy. However, this study was small and did not require p-glycoprotein expression for inclusion. We believe that further clinical trials targeting patients with a functional p-glycoprotein are warranted.

Acknowledgments. We thank Ms. Yumi Ohama and Ms. Mariko Ueki for their excellent technical assistance with the HPLC analysis and Dr. Kenichi Fujita for his valuable comments.

References

1. Hortobagyi GN: Treatment of breast cancer. N Engl J Med (1998) 339: 974-984.
2. Greenberg PAC, Hortobagyi GN, Smith TL, Ziegler LD, Frye DK and Buzdar AU: Long-term follow-up of patients with complete remission following combination chemotherapy for metastatic breast cancer. J Clin Oncol (1996) 14: 2197-2205.
3. Fossati R, Confalonieri C, Torri V, Ghislandi E, Penna A, Pistotti V, Tinazzi A and Liberati A: Cytotoxic and hormonal treatment for metastatic breast cancer: a systematic review of published randomized involving 31,510 women. J Clin Oncol (1998) 16: 3439-3460.
4. Nabholtz JMA, Reese DM, Lindsay MA and Riva A: Docetaxel in the treatment of breast cancer: an update on recent studies. Semin Oncol (2002) 29 (Suppl 12): 28-34.
5. Leonessa F and Clarke R: ATP-binding cassette transporters and drug resistance in breast cancer. Endocr Relat Cancer (2003) 10: 43-73.
6. Seidman AD, Reichman BS, Crown JPA, Yao TJ, Currie V, Hakes TB, Hudis CA, Gilewski TA, Baselga J, Forsythe P, Lepore J, Marks L, Fain K, Souhrada M, Onetto N, Arbuck S and Norton L: Paclitaxel as second and subsequent therapy for metastatic breast cancer: activity independent of prior anthracycline response. J Clin Oncol (1995) 13: 1152-1159.
7. Trock BJ, Leonessa F and Clarke R: Multidrug resistance in breast cancer: a meta-analysis of MDR1/gp170 expression and its possible functional significance. J Natl Cancer Inst (1997) 89: 917-931.
8. Dexter DW, Reddy RK, Geles KG, Bansal S, Myint MA, Rogakto A, Leighton JC and Goldstein LJ: Quantitative reverse transcriptase-polymerase chain reaction measured expression of *MDR1* and *MRP* in primary breast carcinoma. Clin Cancer Res (1998) 4: 1533-1542.
9. Kallio S, Kangas L, Blanco G, Johansson R, Karjalainen A, Perila M, Pippo I, Sundquist H, Sodervall M and Toivola R: A new triphenylethylene compound, Fc-1157a. I. Hormonal effects. Cancer Chemother Pharmacol (1986) 17: 103-108.
10. Kangas L, Nieminen AL, Blanco G, Gronroos M, Kallio S, Karjalainen A, Perila M, Sodervall M and Toivola R: A new triphenylethylene compound, Fc-1157a. II. Antitumor effects. Cancer Chemother Pharmacol (1986) 17: 109-113.
11. Kangas L: Review of the pharmacological properties of toremifene. J Steroid Biochem (1990) 36: 191-195.
12. Rao US, Fine RL and Scarborough GA: Antiestrogens and steroid hormones: substrates of the human p-glycoprotein. Biochem Pharmacol (1994) 48: 287-292.
13. Sonnichsen DS and Relling MV: Clinical pharmacokinetics of paclitaxel. Clin Pharmacokinet (1994) 27: 256-269.
14. Berthou F, Dreano Y, Belloc C, Kangas L, Gautier JC and Beaune P: Involvement of cytochrome P450 3A enzyme family in the major metabolic pathways of toremifene in human liver microsomes. Biochem Pharmacol (1994) 47: 1883-1895.
15. Wurz GT, Emshoff VD, DeGregorio MW and Wiebe VJ: Targeting chemosensitizing doses of toremifene based on protein binding. Cancer Chemother Pharmacol (1993) 31: 412-414.
16. Tominaga T, Hayashi K, Hayasaka A, Asaishi K, Abe R, Kimishima I, Izuo M, Iino Y, Yokoe T, Abe O, Enomoto K, Fujiwara K, Watanabe H, Yamaguchi S, Fukuda M, Yoshida M, Miura S, Miyazaki I, Noguchi M, Senoo T, Sonoo H, Monden Y, Morimoto T, Nomura Y and Tashiro H: Phase I study of NK622 (toremifene citrate). Jpn J Cancer Chemother (1992) 19: 2363-2372 (in Japanese).
17. Shiba E, Watanabe T, Taguchi T, Tsukamoto F and Noguchi S: Plasma concentrations of toremifene citrate and N-desmethyltoremifene in postmenopausal patients with breast cancer. Jpn J Cancer Chemother (2000) 27: 245-249 (in Japanese).
18. Wiebe VJ, Benz CC, Shemano I, Cadman TB and DeGregorio MW: Pharmacokinetics of toremifene and its metabolites in

patients with advanced breast cancer. Cancer Chemother Pharmacol (1990) 25: 247-251.
19. Wiseman LR and Goa KL: Toremifene. A review of its pharmacological properties and clinical efficacy in the management of advanced breast cancer. Drugs (1997) 54: 141-160.
20. DeGregorio MW, Ford JM, Benz CC and Wiebe VJ: Toremifene: Pharmacologic and pharmacokinetic basis of reversing multidrug reisistance. J Clin Oncol (1989) 7: 1359-1364.
21. Wiebe V, Koester S, Lindberg M, Emshoff V, Baker J, Wurz G and DeGregorio M: Toremifene and its metabolites enhance doxorubicin accumulation in estrogen receptor negative multidrug resistant human breast cancer cells. Invest New Drugs (1992) 10: 63-71.
22. Baker WJ, Maenpaa JU, Wurz GT, Koester SK, Seymour RC, Emshoff VD, Wiebe VJ and DeGregorio MW: Toremifene enhances cell cycle block and growth inhibition by vinblastine in multidrug resistant human breast cancer cells. Oncol Res (1993) 5: 207-212.
23. Clarke R, Leonessa F and Trock B: Multidrug resistance/p-glycoprotein and breast cancer: review and meta-analysis. Semin Oncol (2005) 32 (Suppl 7): S9-15.
24. Tolcher AW, Cowan KH, Solomon D, Ognibene F, Goldspiel B, Chang R, Noone MH, Denicoff AM, Barnes CS, Gossard MR, Fetsch PA, Berg SL, Balis FM, Venzon DJ and O'Shaughnessy JA: Phase I crossover study of paclitaxel with r-verapamil in patients with metastatic breast cancer. J Clin Oncol (1996) 14: 1173-1184.
25. Sandor V, Fojo T and Bates SE: Future perspectives for the development of P-glycoprotein modulators. Drug Resist Updat (1998) 1: 190-200.
26. Saeki T, Nomizu T, Toi M, Ito Y, Noguchi S, Kobayashi T, Asaga T, Minami H, Yamamoto N, Aogi K, Ikeda T, Ohashi Y, Sato W and Tsuruo T: Dofequider fumarate (MS-209) in combination with cyclophosphamide, doxorubicin, and fluorouracil for patients with advanced or recurrent breast cancer. J Clin Oncol (2007) 25: 411-417.
27. Seidman AD, Hudis CA, Albanel J, Tong W, Tepler I, Currie V, Moynahan ME, Theodoulou M, Gollub M, Baselga J and Norton L: Dose-dense therapy with weekly 1-hour paclitaxel infusions in the treatment of metastatic breast cancer. J Clin Oncol (1998) 16: 3353-3361.
28. Seidman AD: Single-agent paclitaxel in the treatment breast cancer: phase I and II development. Semin Oncol (1999) 26 (suppl 8): 14-20.
29. Eniu A, Palmieri FM and Perez EA: Weekly administration of docetaxel and paclitaxel in metastatic or advanced breast cancer. Oncologist (2005) 10: 665-685.
30. Pyrhonen SO: Phase III studies of toremifene in metastatic breast cancer. Breast Cancer Res Treat (Suppl) (1990) 16: S41-46.
31. Robinson SP, Parker CJ and Jordan VC: Preclinical studies with toremifene as an antitumor agent. Breast Cancer Res Treat (Suppl) (1990) 16: S9-17.
32. Gams R: Phase III trials of toremifene vs tamoxifen. Oncology (Williston Park) (1997) 11 (Suppl 4): 23-28.
33. Vogel CL: Phase II and III clinical trials of toremifene for metastatic breast cancer. Oncology (Williston Park) (1998) 12 (Suppl 5): 9-13.
34. Gershanovich M, Hayes DF, Ellmen J and Vuorinen J: High-dose toremifene vs tamoxifen in postmenopausal advanced breast cancer. Oncology (Williston Park) (1997) 11 (Suppl 4): 29-36.
35. Hayes DF, Van Zyl JA, Hacking A, Goedhals L, Bezwoda WR, Mailliard JA, Jones SE, Vogel CL, Berris RF, Shemano I and Schoenfelder J: Randomised comparison of tamoxifen and two separate doses of toremifene in postmenopausal patients with metastatic breast cancer. J Clin Oncol (1995) 13: 2556-2566.
36. Asaishi K, Tominaga T, Abe O, Izuo M and Nomura Y: Efficacy and safety of high dose NK 622 (toremifene citrate) in tamoxifen failed patients with breast cancer. Gan to Kagaku Ryoho (Jpn J Cancer Chemother) (1993) 20: 91-99 (in Japanese).
37. Sledge GW Jr, Hu P, Falkson G, Tormey D and Abeloff M: Comparison of chemotherapy with chemohormonal therapy as first-line therapy for metastatic hormone-sensitive breast cancer: an eastern cooperative oncology group study. J Clin Oncol (2000) 18: 262-266.
38. Albain KS, Green SJ, Ravdin PM, Cobau CD, Levine EG, Ingle JN, Pritchard KI, Schneider DJ, Abeloff MD, Norton L, Henderson IC, Lew D, Livingston RB, Martino S and Osborne CK: Adjuvant chemohormonal therapy for primary breast cancer should be sequential instead of concurrent: initial results from intergroup trial 0100 (SWOG-8814). Proc Am Soc Clin Oncol (2002) 21: 143a.
39. Perez EA, Vogel CL, Irwin DH, Kirshner JJ and Patel R: Multicenter phase II trial of weekly paclitaxel in women with metastatic breast cancer. J Clin Oncol (2001) 19: 4216-4223.
40. Gershanovich M, Garin A, Baltina D, Kurvet A, Kangas L and Ellmen J: A phase III comparison of two toremifene doses to tamoxifen in postmenopausal women with advanced breast cancer. Eastern European Study Group. Breast Cancer Res Treat (1997) 45: 251-262.

G Model
IJP-11062; No. of Pages 11

International Journal of Pharmaceutics xxx (2010) xxx–xxx

Contents lists available at ScienceDirect

International Journal of Pharmaceutics

journal homepage: www.elsevier.com/locate/ijpharm

In vitro and *in vivo* anti-tumor effects of novel Span 80 vesicles containing immobilized *Eucheuma serra* agglutinin

Yousuke Omokawa[a], Tatsuhiko Miyazaki[b], Peter Walde[c,**], Koichi Akiyama[d], Takuya Sugahara[e], Seizo Masuda[f], Akihiro Inada[g], Yasuyuki Ohnishi[h], Toshiaki Saeki[i], Keiichi Kato[a,*]

[a] Department of Materials Science and Biotechnology, Graduate School of Science and Engineering, Ehime University, 3 Bunkyo-cho, Matsuyama, Ehime 790-8577, Japan
[b] Department of Pathogenomics, Graduate School of Medicine, Ehime University, Shitsukawa, Toon, Ehime 791-0295, Japan
[c] Department of Materials, ETH, Wolfgang-Pauli-Strasse 10, CH-8093 Zürich, Switzerland
[d] Department of Molecular Structure and Function Analysis, Integrated Center for Sciences, Ehime University, 3-5-7 Tarumi, Matsuyama 790-8566, Japan
[e] Department of Life Science, Faculty of Agriculture, Ehime University, 3-5-7 Tarumi, Matsuyama, Ehime 790-8566, Japan
[f] Department of Bioscience, Integrated Center for Science Shigenobu Station, Ehime University, Shitsukawa, Toon, Ehime 791-0295, Japan
[g] Yamaki Co. Ltd., 1698-6, Kominato, Iyo, Ehime 799-3194, Japan
[h] Central Institute for Experimental Animals, 1430 Nogawa, Miyamae-ku, Kawasaki, Kanagawa 216-0001, Japan
[i] Saitama Medical University International Medical Center, 1397-1 Yamane, Hidaka-city, Saitama 350-1298, Japan

ARTICLE INFO

Article history:
Received 18 November 2009
Received in revised form 15 January 2010
Accepted 19 January 2010
Available online xxx

Keywords:
Liposome
Vesicle
Nonionic
Lectin
Drug delivery
Agglutinin
Span

ABSTRACT

The lectin *Eucheuma serra* agglutinin (ESA) is known from previous studies to specifically bind to high-mannose type *N*-glycans and to induce apoptotic cancer cell death *in vitro*. In this study, Span 80 vesicles, with an average diameter between about 200 and 400 nm, containing immobilized ESA were prepared from the nonionic surfactant Span 80, also known as sorbitan monooleate. The vesicles were investigated *in vitro* and *in vivo* to evaluate the vesicles's potential applicability as novel drug delivery system. The results obtained are promising since the following was observed: (i) vesicular ESA had the same hemagglutinating activity as free ESA, demonstrating its biological activity when bound to the vesicles; (ii) vesicles containing immobilized ESA decreased the viability of Colo201 cancer cells *in vitro* while the growth of normal cells was not affected; (iii) the vesicles showed binding to Colo201 cells *in vitro* and caused inhibition of cancer cell growth in nude mice to which the vesicle-treated cells were added; (iv) the vesicles diminished tumor growth after intravenous administration to nude mice which contained an implanted Colo201 tumor; (v) the vesicles showed a tendency to accumulate at the site of the tumor 6 h after *i.v.* administration to nude mice. Thus, all measurements carried out indicate that this type of Span 80 vesicle can be considered as promising alternatives to conventional phospholipid-based vesicles.

1. Introduction

In recent years there have been numerous investigations of novel drug delivery systems (DDS) for elucidating their applicability as drug carriers for the treatment of various diseases (Allen and Cullis, 2004; Ferrari, 2005; Lian and Ho, 2001; Peer et al., 2007; Couvreur and Vauthier, 2006). Phospholipid vesicles (liposomes), i.e. vesicles composed of natural phospholipids, are often used as DDS (Lian and Ho, 2001; Sharma and Sharma, 1997; Barenholz, 2001; Torchilin, 2005), e.g. for active targeting of specific colon cancer cells (Sato et al., 1988; Koning et al., 2002; Hatziantoniou et al., 2006; Garg et al., 2009). On the other hand, it has been demonstrated that nonionic vesicles prepared from Span 80 have promising physico-chemical properties (high membrane fluidity with temperature dependent fusiogenicity) which make this type of vesicle an attractive possible alternative to the commonly used liposomes (Kato et al., 1993; Kato and Hirata, 1996; Kato and Hirashita, 1997; Ohama et al., 2005; Sugahara et al., 2005). In the food and cosmetic industries, Span 80 is generally known as sorbitan monooleate, although commercial Span 80 is a heterogeneous mixture of sorbitan mono-, di- tri, and tetraesters (Kato et al., 2006).

Span 80 vesicles can be prepared by a recently developed two-step emulsification method which yields vesicles with a membrane composition which is significantly different from commercial Span 80 (Kato et al., 2006). The bilayer membrane of Span 80 vesicles forms under thermodynamic control during the vesicle preparation, with partial elimination of those components present in commercial Span 80 which hinder formation of stable bilayers. Span 80 vesicles have rather fluid membranes; addition of soybean

* Corresponding author. Tel.: +81 976 4686; fax: +81 976 4686.
** Corresponding author. Tel.: +41 44 6320473; fax: +41 44 6321265.
E-mail addresses: peter.walde@mat.ethz.ch (P. Walde), keiichi1017@mc.pikara.ne.jp (K. Kato).

0378-5173/$ – see front matter © 2010 Elsevier B.V. All rights reserved.
doi:10.1016/j.ijpharm.2010.01.033

Please cite this article in press as: Omokawa, Y., et al., *In vitro* and *in vivo* anti-tumor effects of novel Span 80 vesicles containing immobilized *Eucheuma serra* agglutinin. Int. J. Pharm. (2010), doi:10.1016/j.ijpharm.2010.01.033

lecithin and cholesterol (at 9 and 4.5 wt%, respectively) lead to a stabilization of the membrane with a lowering of the membrane permeability (Kato et al., 2008). Furthermore, the two-step emulsification allows the preparation of vesicles with relatively high encapsulation yields for water soluble molecules by entrapping the molecules as inner phase solution, just before the first emulsification is carried out (Figure S1 in Supplementary Material, and Kato et al., 2006; Kato et al., 2008).

Tumor-specific "active targeting" is often achieved by immobilizing tumor-specific ligands such as antibodies, peptides or saccharides onto liposomal drug carrier systems (Peer et al., 2007; Torchilin, 2005; Forssen and Willis, 1998). While most tumor-specific ligands have no intrinsic anti-tumor activity, several lectins are known to possess anti-tumor activity against human cancer cells (Karasaki et al., 2001; Timoshenko et al., 2001; Wang et al., 2000). In this case targeting and anti-tumor activity are combined in one and the same molecule. One particular lectin with such "dual activity" is the lectin *Eucheuma serra* agglutinin (ESA) (Kawakubo et al., 1997). It can be extracted in the two isoforms ESA-1 and ESA-2 from marine red algae (Kawakubo et al., 1997). ESA-1 and ESA-2 have the same molar mass (27,950 g/mol) but differ in isoelectric points (pI = 4.75 for ESA-1 and pI = 4.95 for ESA-2) (Kawakubo et al., 1997). ESA-2 is specific for high-mannose type *N*-glycans (Hori et al., 2007). We have previously shown that ESA has a specific affinity to various cancer cells (specifically to the human colon cancer cell line Colo201), inducing apoptotic cell death *in vitro* (Sugahara et al., 2001) and *in vivo* (Fukuda et al., 2006).

In the work presented we have prepared Span 80 vesicles containing immobilized ESA and measured the activity of these vesicles against tumor cells *in vitro* and *in vivo*. Since ESA has a high affinity to Colo201 cells (see above), these cells were mainly chosen to investigate the tumor targeting properties of the vesicles. Different types of vesicles were prepared as reference systems and the anti-tumor activity of the different types of vesicles was compared by using a number of independent methods.

Contemporary liposomal DDS often contain poly(ethyleneglycol), PEG, immobilized onto the liposome surface. These "PEGylated liposomes", also called "stealth liposomes", generally show a decreased uptake by the reticuloendothelial system (RES), i.e. a prolonged blood circulation time, as compared to conventional liposomes (Couvreur and Vauthier, 2006; Zeisig et al., 1996). For this reason, we also prepared and used for *in vivo* studies PEGylated Span 80 vesicles. The different Span 80 vesicles prepared were as follows (Fig. 1): **CV**, "control vesicles", i.e. Span 80 vesicles without PEGylated lipids or ESA; **PV**, Span 80 vesicles containing PEGylated lipids (DSPE-PEG_{2000}); **EV**, Span 80 vesicles containing immobilized ESA; **EPV**, Span 80 vesicles containing PEGylated lipids and immobilized ESA; **EEPV**, Span 80 vesicles containing PEGylated lipids, immobilized ESA and entrapped ESA.

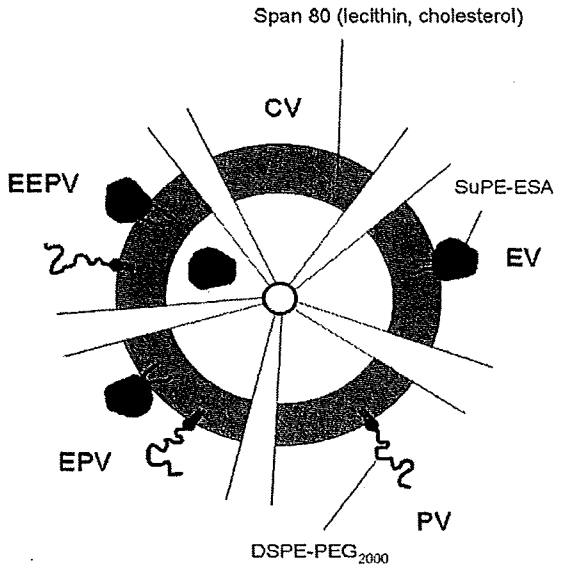

Fig. 1. Schematic representation of the different types Span 80 vesicles used. A cross section through one unilamellar Span 80 vesicle is shown in the center. The composition of the membrane of the different types of vesicles is illustrated. The highly schematic drawing is for an easier distinction of the different types of vesicles, only. The molecular details of the arrangement of the different components are not known. **CV**, Span 80 vesicles without PEGylated lipids or ESA ("control vesicles"); **PV**, Span 80 vesicles containing DSPE-PEG_{2000}; **EV**, Span 80 vesicles containing immobilized ESA; **EPV**, Span 80 vesicles containing DSPE-PEG_{2000} and immobilized ESA; **EEPV**, Span 80 vesicles containing DSPE-PEG_{2000}, immobilized ESA and entrapped ESA.

2. Materials and methods

2.1. Chemicals

Sorbitan monooleate (Span 80) and polyoxyethylene sorbitan monooleate (Tween 80) were purchased from Sigma–Aldrich (St. Louis, MO, USA). Lecithin from soybean was obtained from Wako Pure Chemical Industries (Osaka, Japan) and purified by acetone-precipitation (Inoue, 1974). 1,2-Distearoyl-*sn*-glycero-3-phosphoethanolamine-*N*-[methoxy (polyethyleneglycol)-2000] (DSPE-PEG_{2000}), which is a phospholipid to which a poly(ethyleneglycol) chain with a molar mass of 2000 g/mol is bound, was obtained from NOF Corporation (Tokyo, Japan). Cholesterol was from Wako Pure Chemical Industries.

Isothiocyanic acid octadecylester (IAOE) was synthesized from *N*,*N*-dichlorohexylcarbodiimide (DCCD) and 1-aminooctadecane as follows: In a first vessel, 3.4 g DCCD were first dissolved in 200 mL diethylether, cooled at −10 °C. 8 mL carbon disulphide was then added to this cooled solution. In a second vessel, 4.3 g 1-aminooctadecane were dissolved in 250 mL diethylether, and this solution was added to the cooled DCCD solution. The mixture was left standing at room temperature for 5 h. Afterwards, the solution was filtered using filter paper 5C (Advantec) to remove the byproduct thiourea. The filtrate was evaporated with a rotary evaporator and the obtained oily IAOE product was purified by recrystallization from diethylether.

The lectin ESA (*E. serra* agglutinin, mainly the isoform ESA-2 (Kawakubo et al., 1997) was extracted from the red alga *E. serra* and purified as described previously (Kawakubo et al., 1997). The phospholipid 1,2-dioleoyl-*sn*-glycero-3-phosphatidylethanolamine-*N*-succinyl (SuPE) was obtained from Avanti Polar Lipids (Alabaster, AL, USA). The radioisotope ^{125}I was obtained from MP Biomedicals Inc. (Irvine, CA, USA); ^{125}I was used to isotopically label bovine serum albumin (BSA) with 1,3,4,6-tetrachloro-3α-6α-diphenylglycouril (iodogen), obtained from Pierce Chemical Co. (Rockford, IL, USA). ^{125}I-labeled BSA was prepared as described previously (Hashizume et al., 1990). XRITC (amine-reactive X-rhodamine-5-(and-6)-isothiocyanate) was from Sigma Aldrich. All other reagents used were of guaranteed or biochemical grade.

2.2. Preparation of lipidic ESA-conjugates

The phospholipid-ESA conjugate was prepared as follows: 1 mg/mL of ESA was reacted with SuPE (1.25 mg/mL) in 0.15 M sodium carbonate buffer (pH 9.0) at room temperature. The reaction mixture was incubated for 2 h with vortexing for a few seconds every 30 min, followed by standing at 4 °C for 12 h. Residual SuPE in the buffer solution was removed by gel filtration with a PD-10 column packed with Sephadex G-25 (from Amersham Biosciences).

The IAOE-ESA conjugate was prepared as follows: 10 mg of IAOE was dissolved in 10 μL *N*,*N*-dimethyl sulfonamide (Wako Pure

Please cite this article in press as: Omokawa, Y., et al., *In vitro* and *in vivo* anti-tumor effects of novel Span 80 vesicles containing immobilized *Eucheuma serra* agglutinin. Int. J. Pharm. (2010), doi:10.1016/j.ijpharm.2010.01.033

Table 1
Preparation and characterization of the Span 80 vesicles used in the present study.

Vesicle type (see Fig. 1)	Inner phase: *A* in Figure S1 (Supplementary Material) (0.6 mL)	Content of Tween 80 solution: *B* in Figure S1 (Supplementary Material) (6.0 mL)	Vesicle diameter of refined vesicles (nm)	Vesicles diameter of extruded vesicles (nm)	Phase transition temperature T_m (°C)
CV	PBS	–	187 ± 32	104 ± 7	−40.3
PV	PBS	5.67 mg/mL DSPE-PEG_{2000}	197 ± 12	106 ± 8	−39.6
EV	PBS	18 nmol/mL ESA-SuPE	240 ± 24	100 ± 2	−36.8
EPV	PBS	5.67 mg/mL DSPE-PEG_{2000} + 108 nmol ESA-SuPE	298 ± 30	103 ± 5	−34.7
EEPV	PBS containing ESA (1 mg/mL)	5.67 mg/mL DSPE-PEG_{2000} + 108 nmol ESA-SuPE	362 ± 48	106 ± 6	−38.7

Inner phase, *A*: aqueous solution added at the first emulsification (Figure S1, Supplementary Material).
Tween 80 solution, *B*: aqueous Tween 80 solution at the second emulsification (Figure S1, Supplementary Material).
PBS: phosphate buffered saline (see Section 2).
DSPE-PEG_{2000}: 1,2-distearoyl-*sn*-glycero-3-phosphoethanolamine-*N*-[methoxy (polyethyleneglycol)-2000].
ESA-SuPE: ESA bound to 1,2-dioleoyl-*sn*-glycero-3-phosphatidylethanolamine-*N*-succinyl.

Chemical Industries), following by adding into 1 mg/mL ESA in 0.15 M sodium carbonate buffer. The incubation and purification of the solution were performed with the same manner as that in SuPE conjugation as mentioned above.

2.3. Preparation of Span 80 vesicles

All Span 80 vesicles were prepared with the two-step emulsification method described previously (Kato et al., 2003, 2006, 2008), including slight modifications, as outlined in Figure S1 (Supplementary Material) and described in the following. The incorporation of the lipidic ESA-conjugates into the vesicle membrane was carried out during the second emulsification step (Kato et al., 2003).

Span 80 (264 mg), purified lecithin (24 mg) and cholesterol (12 mg) were first dissolved in 3 mL *n*-hexane. 0.6 mL PBS (phosphate buffered saline composed of 137 mM NaCl, 2.7 mM KCl, 10 mM Na_2HPO_4, 2 mM KH_2PO_4) was added as inner phase, followed by the first emulsification for 6 min at 17,500 rpm using a micro-homogenizer Physcotron NS-310E (Microtec Co. Ltd., Funabashi, Japan). In the case of Span 80 vesicles containing entrapped molecules, the 0.6 mL PBS solution contained either ^{125}I-labeled BSA (about 2000 kcpm), or 1 mg/mL ESA (Table 1). The solvent of the water-in-oil emulsion obtained was evaporated in a rotary evaporator at 28 °C under reduced pressure, yielding a water lipid emulsion to which 6 mL PBS containing 96 mg Tween 80 (1.6 wt%) was added, followed by a mixing with the homogenizer for 2 min at 3500 rpm to obtain the heterogeneous Span 80 vesicle suspension. Depending on the type of vesicles prepared (Table 1), this Tween 80 solution contained the phospholipid-ESA conjugate, the IAOE-ESA conjugate, or DSPE-PEG_{2000}. The heterogeneous vesicle suspension was stirred with a magnetic stirrer for 3 h at room temperature, followed by storage overnight at 4 °C. The vesicles were then purified by ultracentrifugation (50,000 rpm at 4 °C for 240 min) in a Himac centrifuge CR15B (Hitachi Koki Co. Ltd., Tokyo, Japan) and the lower phase was purified by gel filtration on a 7 cm (diameter) × 50 cm (length) column containing Biogel-A5m (Bio-Rad Laboratories, Richmond, CA, USA). In comparison to our earlier description (Kato et al., 2006), gel filtration was used instead of dialysis to obtain the refined vesicle suspension. As shown previously by a HPLC analysis (Kato et al., 2006; Kato et al., 2008), the content of Tween 80 in the final vesicle preparation was negligibly small.

Polycarbonate membrane extrusions of all vesicle suspensions were carried out as described previously (Kato et al., 2008).

2.4. Characterization of Span 80 vesicles

The size of the vesicles was analyzed by dynamic light scattering (DLS) using a DLS-6000EW instrument (Otsuka Electronics Co. Ltd., Osaka, Japan) equipped with a 10 mW He–Ne laser source (632.8 nm); the polydispersity index was between 0.17 and 0.20. For the DLS measurements the vesicle suspension was diluted with PBS.

The morphology of the vesicles was analyzed by transmission electron microscoy (TEM) and the phase transition temperature (T_m) were determined as described before (Kato et al., 2008).

The amount of ESA immobilized on the Span 80 vesicles was determined with the Lowry method (Lowry et al., 1951).

2.5. Hemagglutinating test

The activity of the immobilized ESA was analyzed by assaying its hemagglutinating activity against sheep erythrocytes because it is known that free ESA exhibits hemagglutinating activity against sheep and trypsinized rabbit red blood cells (Kawakubo et al., 1997). The hemagglutinating activity assay was performed in a 2% (v/v) erythrocyte suspensions, as described previously (Kawakubo et al., 1997). The hemagglutinating activities of the Span 80 control vesicles (**CV**), of free ESA, and of Span 80 vesicles containing immobilized ESA (**EV**) were compared by considering the lowest concentration exhibiting positive agglutination as the titer of the activity.

2.6. Cells

Human colon cancer cell line Colo201 (ATTC#CCL-224) and human breast cancer cell line MCF-7 (ATCC#HTB-22) were obtained from ATTC (American Type Cell Collection, Manassas, VA, USA). Murine colon cancer cell line Colon26 derived from BALB/c mouse, were provided by the Institute of Development, Aging and Cancer, Tohoku University (Sendai, Japan). Human non-cancerous mammary epithelial cell line MCF10-2A was purchased from ATCC (Rockville, MD, USA). The cancer cells were cultured in E-RDF medium® (Kyokuto Pharmaceutical Industrial Co., Ltd., Tokyo, Japan) containing 10% fetal bovine serum (FBS) under humid conditions with 5% CO_2 at 37 °C in a CO_2 incubator. MCF10-2A cells were cultured in 10% FBS-E-RDF medium supplemented with 500 ng/mL of hydrocortisone and 20 ng/mL of epidermal growth factor (EGF) under the same culture condition of Colo201.

2.7. In vitro cytotoxicity test

Colo201 cells (1×10^5 cells/mL) were cultured on 48-well plate filled with 0.5 mL of 10% FBS-contained E-RDF medium. The cells were washed with PBS, and incubated for 24 h with 0.5 mL of 10% FBS-E-RDF medium containing the following one of the reagents: phosphate buffered saline (PBS) as a non-vesicle control; Span 80 control vesicles (**CV**: $OD_{600\,nm}$ = 0.260); or Span 80 vesicles containing immobilized ESA (**EV**: $OD_{600\,nm}$ = 0.260). The ESA-concentration

Please cite this article in press as: Omokawa, Y., et al., *In vitro* and *in vivo* anti-tumor effects of novel Span 80 vesicles containing immobilized *Eucheuma serra* agglutinin. Int. J. Pharm. (2010), doi:10.1016/j.ijpharm.2010.01.033

in the vesicle suspension was 0.054 mg/mL). After incubation, the cells were harvested, and washed twice with PBS, then resuspended in 1 mL of PBS. The viability of the cells in the suspension was evaluated with the trypan blue dying method (Gortzi et al., 2003; Konopka et al., 1996). Similarly, the cytotoxicity of **CV** and **EV** against MCF10-2A cells was also analyzed. A phase contrast microscopy analysis of Colo201 cells treated with **EV** was also performed, as outlined in the following: Colo201 cells and MCF10-2A cells were incubated for 12 h in E-RDF medium containing 10 vol% FBS and 1 vol% **EV**. After incubation, these cells were observed with a phase contrast microscope.

2.8. In vitro apoptosis test

DNA was extracted from Colo201 cells which were incubated in the presence of **EV** for 8 h, then electrophoresed in a 2% agarose gel to detect DNA laddering associated with apoptosis (Sugahara et al., 2001; Martin et al., 1995; Ioannou and Chen, 1996; Shirai et al., 2009).

2.9. In vitro cell binding test

In order to visualize the affinity of ESA to cancerous cells, a specific binding test was performed. ESA was first labeled with XRITC, a red fluorescence reagent, followed by addition of the XRITC-labeled ESA to Span 80 vesicles. These vesicles were then incubated with Colo201, MCF7, and MCF10-2A cells for a few minutes. Afterwards, micrographs were captured with a fluorescent microscope IX-FLA (Olympus corp., Tokyo, Japan).

2.10. Animal studies

Female Balb/*c-nu/nu* mice and female Balb/cByjJcl mice (4 weeks old) were purchased from Clea Japan Inc. (Tokyo, Japan). Human colon cancer cell line Colo201 or murine colon cancer cell line Colon26 ($1.0–5.0 \times 10^6$ cells per mice) were subcutaneously transplanted into 6 weeks old female Balb/c-*nu/nu* and Balb/cByjJcl mice, respectively; Colo201 cells from human are difficult to transplant into a mouse with normal immunocompetence. All the animal experimental protocols were in accordance with the Guide for Animal Experimentation, Ehime University, and approved by the Committee for Animal Experimentation, Ehime University.

2.11. Biodistribution analysis

BSA (50 μL, 5 mg/mL) was first labeled with the radioisotope ^{125}I (50 μL, 2 mCi/mL) with the iodogen method as described previously (Hashizume et al., 1990). Although iodine is specifically uptaken by the thyroid gland for the formation of the thyroid hormone, the labeling method has been often used for preparing a radioactive tracer in previous studies (Kuan et al., 1999; Foulon et al., 2000; Korde et al., 2000; Larsson et al., 2001). In this experiment, ^{125}I-BSA was used as a model molecule to monitor the biodistribution of the aqueous content of the vesicles.

^{125}I-BSA was encapsulated into four types of Span 80 vesicles, **CV**, **PV**, **EV** and **EPV**. After the preparation, the concentration of these vesicles was regulated to about 2000 kcpm based on the radioactivity of ^{125}I per 200 μL. These vesicles were intravenously injected into BALB/cA-*nu/nu* mice with transplanted Colo201, of which the tumor volume was approximately 1000 mm^3. The concentration of the injected vesicle suspension was about 2000 kcpm of dose (approximately $(2–5) \times 10^{11}$ vesicle particles/mL suspension). At 1, 3, 6 and 24 h after injection, the amount of radioactivity in the tumors, and in various organs and in the blood was measured using a well-type gamma counter ARC-3000 (Aloka, Tokyo, Japan). The accumulation amount in each tissue is represented as a "percentage of dose" calculated by Eq. (1).

$$\text{percentage of dose (\%)} = \frac{\text{radiation dose in tissue (cpm)}}{\text{radiation dose injected vesicle sample (cpm)}} 100 \quad (1)$$

2.12. In vivo anti-tumor activity test

In order to prepare tumor-bearing mice, Colo201 cells ($1–5 \times 10^6$ cells) were subcutaneously transplanted into the back of nude mice. When the tumor volume reached to 100–300 mm^3 a few weeks after the transplantation, **EPV**s or **EEPV**s (0.01 mL/g body weight) were intraperitoneally or intravenously injected every 3 days up to 15 days. Throughout the experiments, the tumor size and body weight of the mice were measured. The longest tumor diameter (length d_1) and the diameters crossing the longest diameters at right angles (widths d_2) were measured with a slide caliper, then the tumor volumes (V) were calculated according to the following equation $V(mm^3) = d_1\,(mm) \times d_2\,(mm) \times d_2\,(mm)/2$ (Rad et al., 2007). The values of body weight and tumor volume at any time were divided by the body weight and the volume at the start of injection (day 0), respectively, to obtain normalized values. These values are represented as relative body weight (W_{mr}) and relative tumor volume (V_{tr}). In order to determine the anti-tumor activity, the tumor growth inhibition was defined as the ratio of the median tumor volume for the treated *vs.* control group (T/C) with the following Eq. (2), according to Rad et al. (2007).

$$\text{T/C (\%)} = \frac{\text{median tumor volume of treated group at day } X\ (mm^3)}{\text{median tumor volume of control group at day } X (mm^3)} 100 \quad (2)$$

The T/C value was used to evaluate of the anti-tumor effect of the samples at the terminal point of the logarithmic growth phase of the murine tumor. These measurement methods were applied in all other mouse experiments.

2.13. In vivo apoptosis test

Three days after the *i.v.* injection of **EPV**, the tumors were excised from the Colo201 tumor-bearing BALB/cA-*nu/nu* mice, and formalin-fixed paraffin-embedded tissue sections were subsequently prepared for *in situ* apoptosis detection by terminal deoxynucleotidyl transferase-mediated dUTP nick end labeling (TUNEL) using the In Situ Apoptosis Detection Kit (Takara Biomedicals, Shiga, Japan) (Fukuda et al., 2006) and immunohistochemistry with anti-single-stranded DNA antibody (DAKO Japan, Kyoto Japan).

2.14. Internalization test

The delivery of water soluble molecules encapsulated inside **EPV** to the tumor in mice was analyzed. **EPV** containing encapsulated fluorescein isothiocyante (FITC) were intravenously injected to mouse (BALB/cByJJCl, 6 week olds, female) with about 500 mm^3 volume of colon tumor from mouse colon cancer cell line Colon26. At 0, 3, 6 and 24 h after the injection, the murine tumor was resected from the mouse. The tumor was quickly frozen in dry ice/acetone bath (about −80 °C), and then sliced to 5 μm thin sections with a microtome (Cryostat HM520). The section was fixed in Morphosave (Ventana Medical Systems, Tucson, AZ) for 15 min, and observed with a fluorescence microscope IX-FLA.

Please cite this article in press as: Omokawa, Y., et al., *In vitro* and *in vivo* anti-tumor effects of novel Span 80 vesicles containing immobilized *Eucheuma serra* agglutinin. Int. J. Pharm. (2010), doi:10.1016/j.ijpharm.2010.01.033

Table 2
Immobilization of ESA onto Span 80 vesicles.

Lipid anchor	Added amount of lipid anchor (μmol)[a]	Added amount of ESA (μg)[b]	Amount of immobilized ESA (μg)	ESA immobilization efficacy (%)[c]
–	–	250	12	4.7
IAOE	32.1	250	56	22
SuPE	2.9	250	121	48

[a] The values given are the amounts of lipid anchor added per 50 nmol ESA.
[b] Amount of ESA added (250 μg) per 132 mg Span 80.
[c] Percentage of immobilized ESA with respect to the amount of ESA added.

2.15. Statistical analysis

The statistical analysis of significancy between the data from two groups was performed using Student's *t*-test. Multiple comparisons were performed using the analysis of variance (ANOVA) with Statcel® (OMS publishing Inc., Saitama, Japan). The significancy was designated at $P < 0.05$.

3. Results

3.1. Preparation and characterization of the Span 80 vesicles

All Span 80 vesicles used in the study were prepared by the two-step emulsification method, as outlined in Figure S1 in Supplementary Material. For the vesicles containing PEGylated lipids (**PV, EPV, EEPV**) and for the vesicles containing ESA (**EV, EPV, EEPV**) DSPE-PEG_{2000} and ESA-SuPE were added before the second emulsification (Table 1 and Figure S1 in Supplementary Material).

Immobilization of ESA on the Span 80 vesicles occurred most efficiently if ESA was bound to SuPE (Table 2), i.e. if the ESA-SuPE conjugate was used. Vesicle binding of ESA alone was low; the immobilization efficacy was only 4.7% (Table 2). In the case of IAOE as anchor lipid, the immobilization efficacy was 22%, as compared to 48% if SuPE was used as lipid anchor (Table 2). Based on these immobilization trials, for all further measurements, ESA was immobilized onto Span 80 vesicles as ESA-SuPE conjugate.

The immobilized amounts of ESA and PEGylated lipid per Span 80 (based on an average Span 80 molecular mass of 737 g/mol, see Kato et al., 2006; Kato et al., 2008), were $(5.0 \pm 0.4) \times 10^{-5}$ mol% and $(3.1 \pm 0.6) \times 10^{-2}$ mol%, respectively.

The average sizes of the refined vesicles prepared were determined by DLS (Table 1). The diameters varied between about 200 nm and 400 nm. The polydispersity of the vesicles was relatively high, as can be seen also from the transmission electron micrographs shown in Fig. 2. The average size and the polydispersity of the vesicles could be reduced by passing the vesicle suspension through polycarbonate membranes with 100 nm pore diameters. The resulting vesicles had diameters of about 100 nm (Table 1).

The phase transition temperature of the different vesicle preparations was in the range of −35 to −40 °C (Table 1), in agreement with what we determined previously (Kato et al., 2008). The membrane of the vesicles at room temperature was therefore rather fluid in all cases.

3.2. Hemagglutinating activity of *EV*

To investigate the bioactivity of the immobilized ESA, the hemagglutinating activity of the Span 80 vesicles containing immobilized ESA (**EV**) was measured against sheep red blood cells and compared with the hemagglutinating activity of free ESA. Both, free ESA and **EV** showed the same activity (2.86 ng/mL). Both PBS alone and Span 80 vesicles without ESA (**CV**) did not show hemagglutinating activity. These results indicate that ESA could be immobilized under retention of its biological activity.

3.3. In vitro cytotoxicity and apoptotic behavior of *EV*

To detect a possible anti-tumor activity of **EV**, the cytotoxicity of **EV** against Colo201 was evaluated and compared with the activity of **CV**. The time-course of the cell viability is shown in Fig. 3. **EV** clearly showed a stronger cytotoxicity than **CV**. The viability of the Colo201 cells decreased to 17.2 ± 6.3% after 24 h

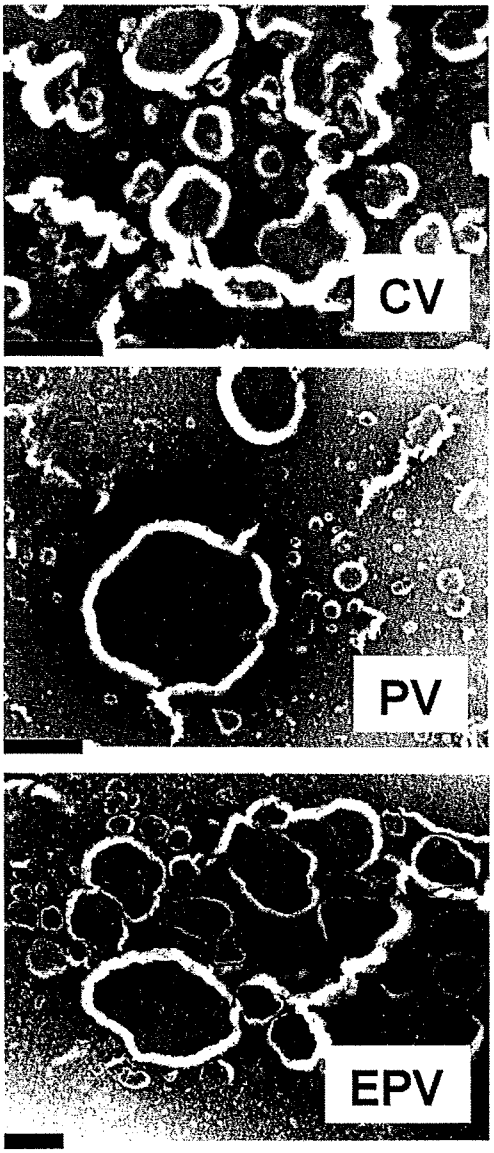

Fig. 2. Transmission electron micrographs (TEM) of Span 80 vesicles (**CV**), of Span 80 vesicles containing DSPE-PEG_{2000} (**PV**), and of Span 80 vesicles containing DSPE-PEG_{2000} and immobilized ESA (**EPV**). Negative staining method; length of the bar: 500 nm.

Please cite this article in press as: Omokawa, Y., et al., *In vitro* and *in vivo* anti-tumor effects of novel Span 80 vesicles containing immobilized *Eucheuma serra* agglutinin. Int. J. Pharm. (2010), doi:10.1016/j.ijpharm.2010.01.033

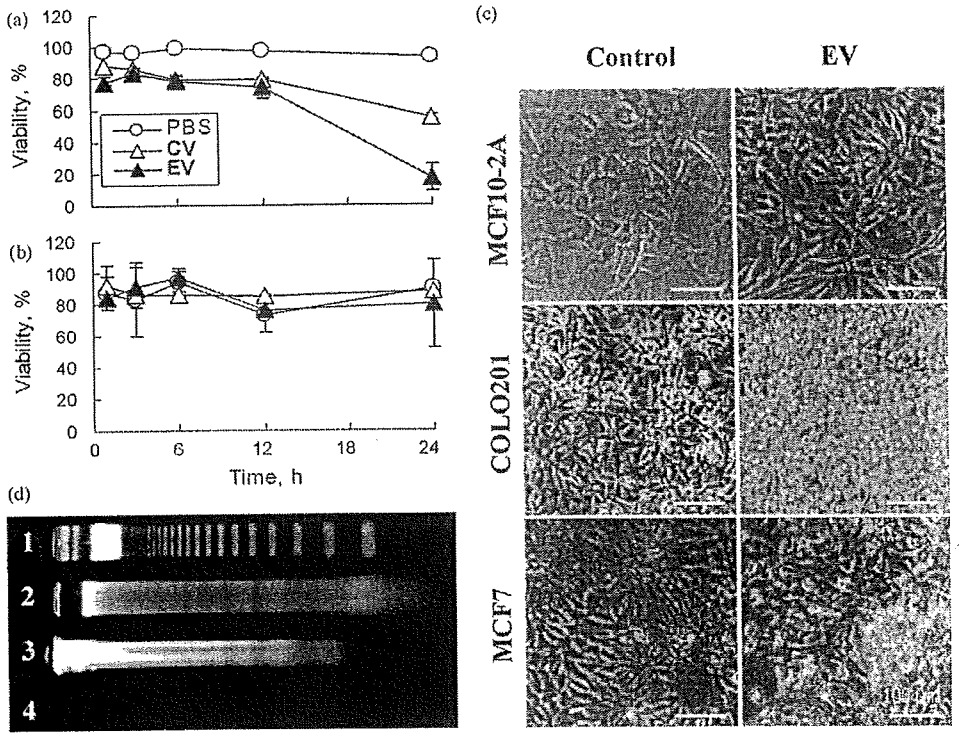

Fig. 3. (a) and (b) Time-course of the viability of Colo201 cells (a) and of MCF10-2A cells (b), number of independent measurements: $n = 2$ (c) Phase contrast micrographs of Colo201, MCF7 and MCF10-2A cells treated with **EV**. These cells were incubated for 12 h in E-RDF medium containing 10 vol% FBS and 1 vol% **EV** (OD_{680} = 0.046). Magnification: ×200. (d) Fragmentation of the DNA of Colo201 cells (lane 2), MCF7 cells (lane 3) and MCF10-2A cells (lane 4) treated with Span 80 vesicles containing immobilized ESA (**EV**) (lower lane). Lane 1: DNA ladder marker.

incubation while the cell viability in the presence of **CV** decreased to 55.1 ± 5.6% in the same period of time under the conditions used (Fig. 3a). On the other hand, these vesicles showed no effect on the viability of normal cells, MCF10-2A (Fig. 3b). The phase contrast microscopic observation of these cells after **EV**-treatment showed that morphological changes of the Colo201 and MCF7 cells (tumor cells) were induced, while there were no changes in the case of MCF10-2A cells (normal cells) (Fig. 3c). Our previous study indicated that ESA-treatment excites the Capase3 activity of Colo201 cells (Sugahara et al., 2001). Therefore, the morphological change of Colo201 cells treated with **EV** is considered to be associated with apoptosis. Moreover, we have already reported (Sugahara et al., 2001) that free ESA specifically combines with many tumor cells such as Colo201, HeLa and MCF7, inducing apoptotic death of the cancer cells, while free ESA did not combine with MCF10-2A significantly (from flow cytometric measurements) and did not injure the cell. These results suggest that ESA immobilized on **EV** also preferentially injures the cancer cells with high-mannose-type sugar chains (such as Colo201 and MCF7 cells).

The DNA fragmentation ("DNA laddering") in Colo201 cells treated with **EV** was determined by gel electrophoresis (Fig. 3d), as described previously (Sugahara et al., 2001). On the other hand, DNA fragmentation in human breast cancer cell line MCF7 was also detected, but not in the case of MFC10-2A (Fig. 3d). In our earlier study it was shown that ESA is toxic against human cancer cell lines (colon, uterine cervix, and breast) (Sugahara et al., 2001). The mechanism responsible for the ESA cytotoxicity involves the binding of ESA to the carbohydrates on the surface of the cells, which leads to an induction of apoptotic cell death as indicated by DNA laddering (Sugahara et al., 2001). The observed DNA laddering in the case of **EV** indicates that not only free ESA but also ESA which is immobilized onto Span 80 vesicles induces apoptotic cell death in colon cancer cell lines.

3.4. *In vitro* binding of **EV** to cancer cells

For investigating the affinity of **EV** to colon cancer cells, a fluorescent test for tumor cell binding was used by applying Span 80 vesicles containing immobilized XRITC-labeled ESA. ESA was first labeled with XRITC and then immobilized onto the vesicles to yield **XRITC-EV** (without preparation of a lipidic conjugate). Since XRITC is a hydrophobic red fluorescent dye, binding of XRITC-ESA is expected to be more efficient than ESA alone as shown in Table 2.

Colo201, MCF7, and MCF10-2A cells were incubated with **XRITC-EV** for a few minutes and then observed with the fluorescence microscope. The microphotographs are shown in Fig. 4a–f. Fluorescence was observed in Colo201 cells and MCF7 cells (Fig. 4d and e). There was no fluorescence in the MCF10-2A cells (Fig. 4f). These results indicate that Span 80 vesicles containing immobilized ESA binds to cancer cells Colo201 as well as to the cancer cells MCF7, but not to the normal cells MCF10-2A. As shown previously, ESA cell binding occurs *via* interactions between ESA and specific carbohydrates present on the surface of cancer cells (Sugahara et al., 2001). The cancer cell binding property of free ESA (Sugahara et al., 2001) remained if ESA was immobilized onto Span 80 vesicles (Fig. 4d and e).

3.5. *Biodistribution of the vesicles*

Prior to the *in vivo* anti-tumor activity tests in mice, we investigated whether *i.v.* administrated Span 80 vesicles containing immobilized ESA are preferentially taken up by the tumor, or whether there is no tumor specificity of the vesicles containing ESA. Furthermore, since liposomal DDS often contain PEGylated lipids to decrease uptake by the RES (Allen, 1994; Zeisig et al., 1996; Maruyama et al., 1997; Gabizon et al., 1997; Couvreur and Vauthier, 2006), Span 80 vesicles containing immobilized ESA *and* PEGylated

Please cite this article in press as: Omokawa, Y., et al., *In vitro* and *in vivo* anti-tumor effects of novel Span 80 vesicles containing immobilized *Eucheuma serra* agglutinin. Int. J. Pharm. (2010), doi:10.1016/j.ijpharm.2010.01.033

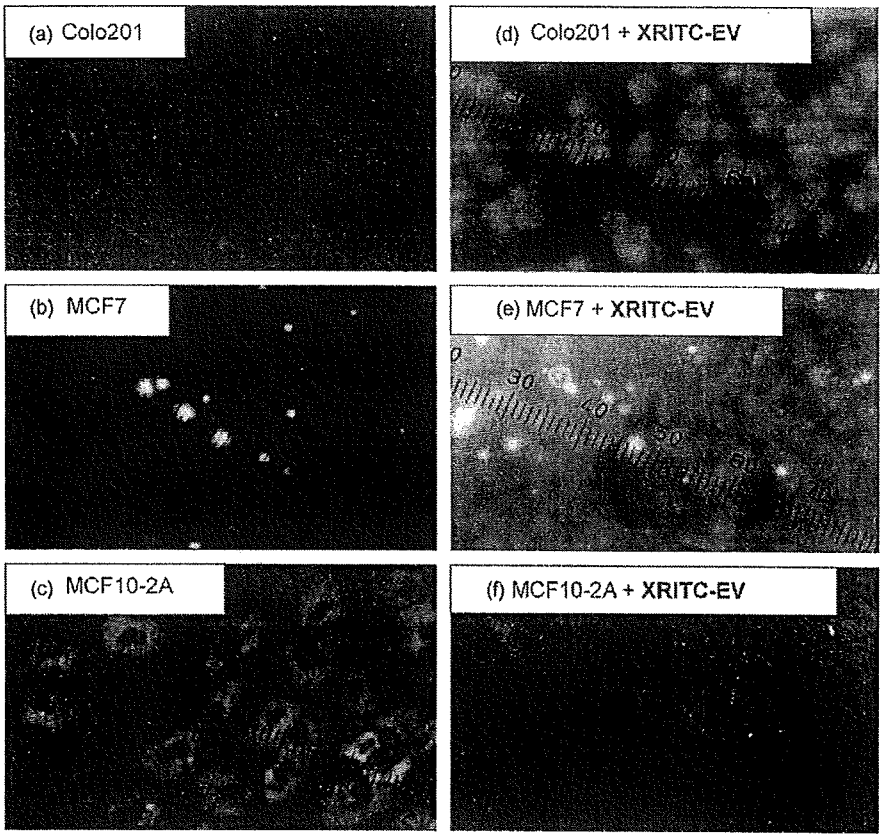

Fig. 4. Fluorescence micrographs of three types of cells before and after treatment with Span 80 vesicles containing immobilized XRITC-ESA (**XRITC-EV**). (a–c) Untreated cells; (d–f) cells after treatment with **XRITC-EV**. The cells used were Colo201 (a and d), MCF7 (b and e), and MCF-10-2A (c and f).

lipids (**EPV**) were prepared, and their *in vivo* behavior was directly compared with **EV** and **PV**. The vesicles were loaded with ^{125}I-BSA, and the delivery of ^{125}I-BSA encapsulated inside **EPV, EV** or **PV** was investigated by examining the biodistribution of ^{125}I-BSA in the nude mice bearing a Colo201 tumor. The accumulated amount of ^{125}I-BSA was evaluated based on the measured radioactivity and using Eq. (1). The results of this biodistribution experiment are shown in Figs. 5 and 6.

At 6 h after *i v.* injection, the tumor uptake of ^{125}I-BSA encapsulated in **EV** and **EPV** was by trend higher as compared to the uptake of ^{125}I-BSA encapsulated in **PV** and **CV** (Fig. 5). The uptake of ^{125}I-BSA in **EV** and **EPV** increased in the range of 1–6 h, while the uptake of ^{125}I-BSA in **CV** decreased (Fig. 5). On the other hand, immediately after *i.v.* injection, the uptake of ^{125}I-BSA in **PV, EV** and **EPV** by the liver, kidney and spleen was lower than the uptake of ^{125}I-BSA in **CV** (Fig. 6a–c). Fig. 6 shows that the lower uptake by the RES cannot be correlated with the presence of PEG in the vesicles. Therefore, there is no evidence (Fig. 6b) for the existence of a "stealth effect" caused by PEG in the case of Span 80 vesicles containing immobilized ESA. It seems that the presence of ESA in **EV**, without any PEGylated lipids, already lowers vesicle uptake by the RES.

In any case, the presence of PEGylated lipids in **EPV** did not significantly alter the biodistribution of the ESA-containing Span 80 vesicles. Furthermore, ESA was still biologically active in the presence of PEGylated lipids (Figs. 7 and 8). However, if specific antibodies against ESA are produced by the repeated injection of **EV** or **EPV** *in vivo*, the PEG on the **EPV** surface may inhibit the binding of the antibodies to ESA.

Although the number of mice used in the experiments reported in Fig. 5 was low (Table S1, Supplementary Material), there is a trend that ^{125}I-BSA encapsulated in **EV** or **EPV** is more efficiently taken

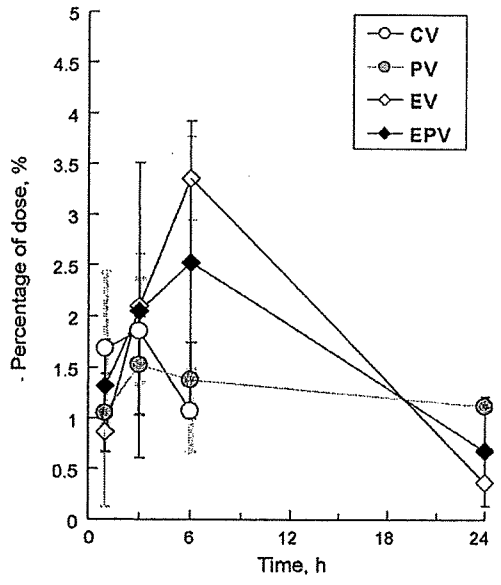

Fig. 5. Tumor accumulation in the BALB/cA-*nu/nu* mice bearing Colo201 tumors by using Span 80 vesicles containing entrapped ^{125}I-BSA (2000 kcpm). The Span 80 vesicles used were **CV** (opened circle), **EV** (opened rhombus), **PV** (closed circle) and **EPV** (closed rhombus). The vesicles were injected intravenously and the uptake of ^{125}I-BSA in the tumor tissue was measured at 1, 3, 6, and 24 h after injection. Mean values (±S.D.) are given for measurements carried out with 2–3 animals/experimental group. It was not possible to us to perform the experiments with a higher number of mice. Details about animal number used in these experiments are shown in Table S1 in Supplementary Material.

Please cite this article in press as: Omokawa, Y., et al., *In vitro* and *in vivo* anti-tumor effects of novel Span 80 vesicles containing immobilized *Eucheuma serra* agglutinin. Int. J. Pharm. (2010), doi:10.1016/j.ijpharm.2010.01.033

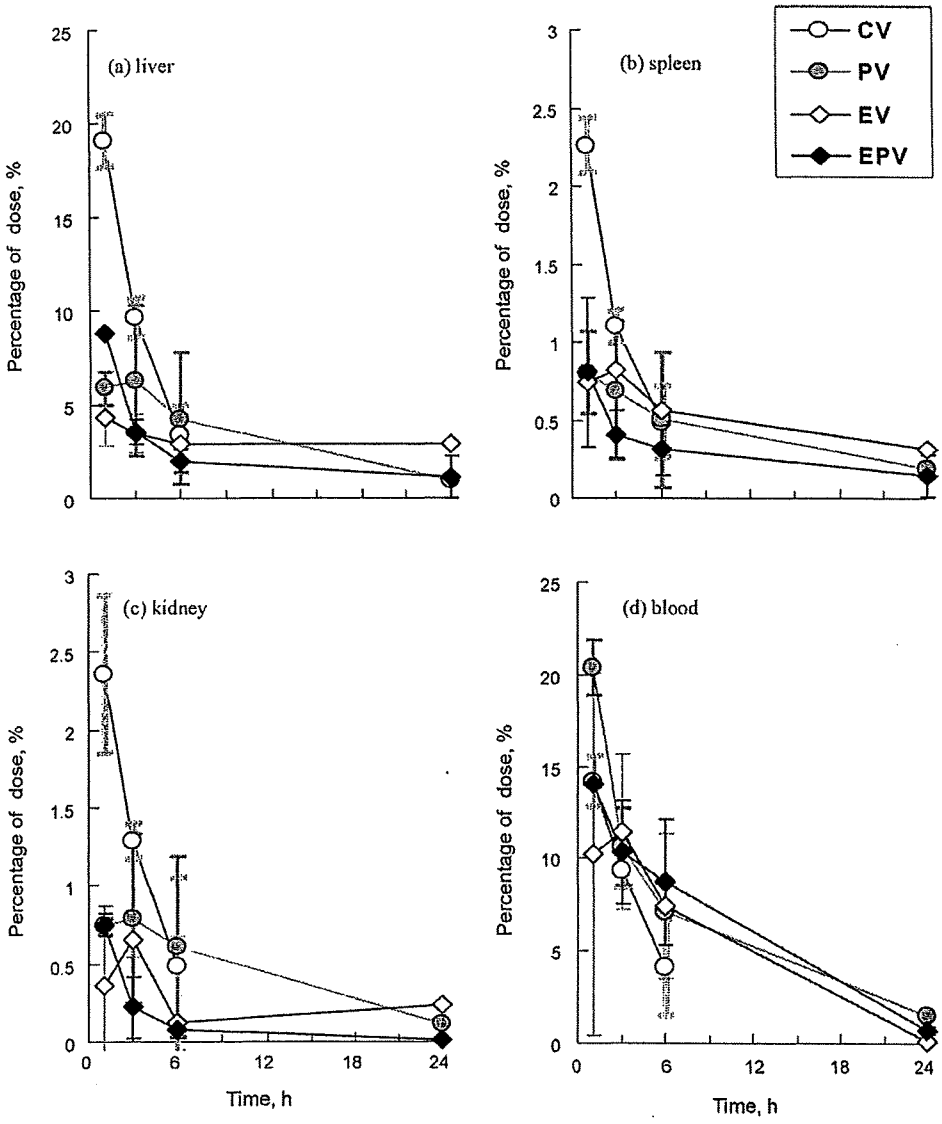

Fig. 6. Biodistribution of ^{125}I-BSA in Colo201 tumor-bearing BALB/*cA-nu/nu* mice after intravenous injection of Span 80 vesicles containing ^{125}I-BSA (2000 kcpm). The Span 80 vesicles used were **CV** (opened circle), **EV** (opened rhombus), **PV** (closed circle) and **EPV** (closed rhombus). The uptake of ^{125}I-BSA by liver (a), spleen (b), kidney (c) and in the whole blood (d) was measured at 1, 3, 6, and 24 h after injection. The time courses of the uptake of ^{125}I-BSA in the tumor are shown in Fig. 5. Mean values (±S.D.) are given for measurements carried out with 2–3 animals/experimental group. Details about animal number used in these experiments are shown in Table S1 in Supplementary Material.

up by the tumor than ^{125}I-BSA encapsulated in **PV** or **CV**. This is most likely due to specific interactions between ESA immobilized on **EV** or **EPV** and the carbohydrate chains on the surface of the tumor cells, as shown previously in an *in vitro* study using free ESA (Sugahara et al., 2001).

Recently, we found that **EPV** injected into Colon26 tumor burden mouse (Balb/cByjJcl) showed higher anti-tumor activity as compared to **EV** (data not shown). The results of this study will be presented in a forthcoming paper (in preparation). The difference in the anti-tumor activity between **EV** and **EPV** may be caused by a hindrance of the ESA-anti-ESA antibody binding by the PEG chains; anti-ESA antibodies are expected to be produced in the mouse upon repeated administration of **EV** or **EPV**. This means that **EV** are more rapidly removed *via* binding to anti-ESA antibodies than **EPV**. Therefore, the modification of the Span 80 vesicle with ESA *and* PEG is at the end expected to enhance the anti-tumor effect of **EPV**. For this reason, **EPV** was used instead of **EV** in the *in vivo* anti-tumor activity tests described in the following section.

3.6. Anti-tumor activity of *EPV* on Colo201 cancer xenografts in vivo

EPV was administered into Colo201 tumor-bearing mice, followed by a measurement of the weight of the mice and the volume of the tumor. The time-course of the relative body weight (W_{mr}) and of the relative tumor volume (V_{tr}) of the mice to which **EPV** was administrated *i.v.* (ESA-dose 2.0 μg/g-mouse-weight) is shown in Fig. 7, together with the corresponding values for **EEPV** (ESA-dose 2.5 μg/g-mouse-weight) and PBS as a control. In all three cases, W_{mr} increased similarly, suggesting that **EPV** and **EEPV** did not cause general toxicity in the mice.

The particle size of conventional PEGylated liposomes used *in vivo* is usually around 100 nm. From our previous studies (Kato et al., 2006; Kato et al., 2008), it was revealed that the membrane fluidity of Span 80 vesicles is considerably higher as compared to the fluidity of the membrane of conventional phospholipid vesicles. Therefore, Span 80 vesicles may more easily migrate through the

Please cite this article in press as: Omokawa, Y., et al., *In vitro* and *in vivo* anti-tumor effects of novel Span 80 vesicles containing immobilized *Eucheuma serra* agglutinin. Int. J. Pharm. (2010), doi:10.1016/j.ijpharm.2010.01.033

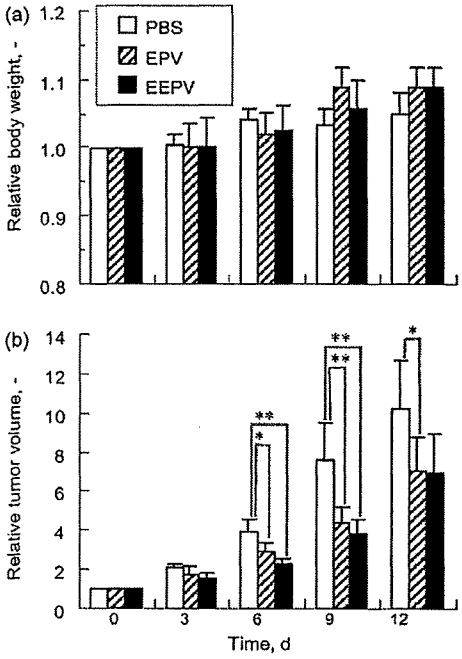

Fig. 7. Time courses of body weight of the mice (W_{mr}) and relative tumor volume (V_{tr}) of the nude mice bearing Colo201 tumors to which **EPV** or **EEPV** were injected. The amounts of ESA in **EPV** and in **EEPV** were 2.0 and 2.5 μg/mL, respectively. The day of vesicle injection is defined as day 0. Mean values (±S.D.) of W_{mr} and V_{tr} are shown with standard deviation (n = 5–10).

pore structure of the blood vessel wall near the tumor by fluctuating changes of the vesicle shape. Thus, it was revealed that administration of Span 80 vesicle with a particle size between 200 and 400 nm, easily prepared without extrusion, is effective enough for the treatment of the tumors. The fluidity of Span 80 vesicles can be seen as an advantage in this respect.

As shown in Fig. 7b, V_{tr} in the case of **EPV**- and **EEPV**-treated mice were lower than in the case of the control mice. In other *in vivo* experiments, the T/C values in the **EPV**- and **EEPV**-injected groups (on the 9th day) were 58.0 ± 4.3% and 51.1 ± 4.2%, respectively. The results suggested that the tumor growth inhibition effects of **EPV** and **EEPV** were basically due to the immobilized ESA and encapsulated-ESA. The findings are also supported by the result from a *semi in vivo* experiment as follows. Colo201 cells treated with **EV** could not be transplanted onto Balb/c-*nu/nu* mice at all, although Colo201 cells treated with **CV** or PBS could be transplanted (Figure S2, Supplementary Material). These results indicate that **EPV** and **EEPV** exhibited significant anti-tumor activity *in vivo* without addition of any of the known anti-cancer agents.

Furthermore, there was no indication of an allergic reaction possibly caused by the vesicle components. Please note that in the final Span 80 vesicle preparation the content of Tween 80, used during the second emulsification stage (Figure S1, Supplementary Material), was negligibly small (Kato et al., 2006).

3.7. *EPV administration induced apoptosis in transplanted Colo201 tumors*

To clarify whether the **EPV** administration induces apoptosis in tumor cells in the same manner as free ESA does, we analyzed the

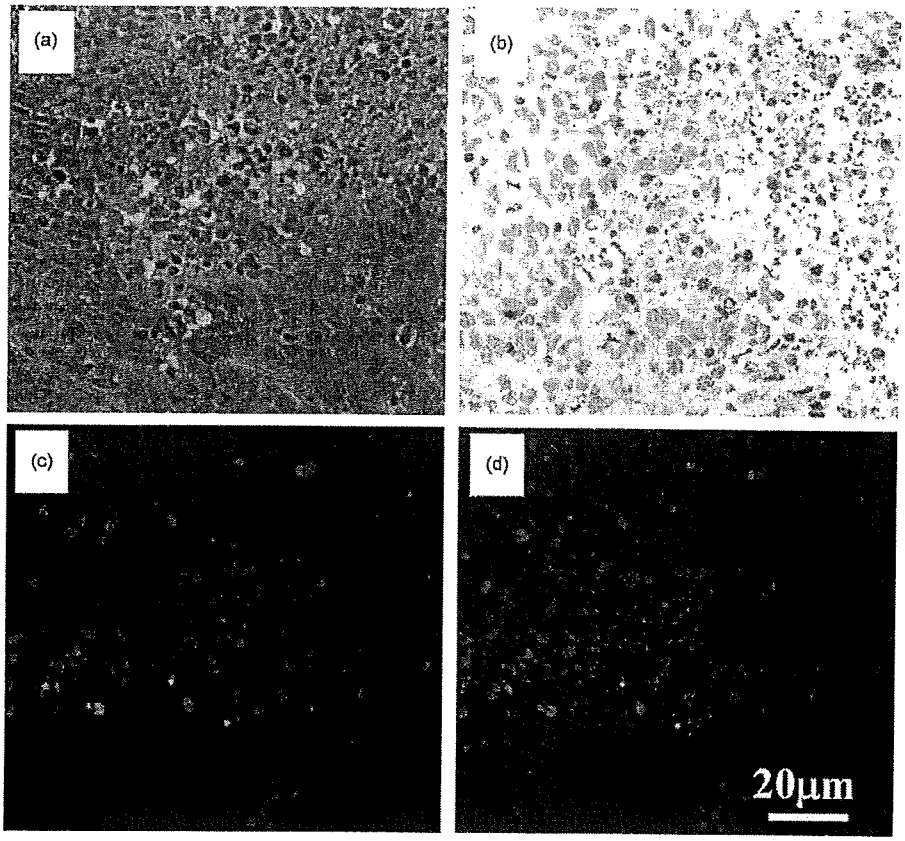

Fig. 8. Apoptosis of Colo201 tumor cells in mice at 72 h after intravenous administration of **EPV** in nude mice bearing Colo201 tumors: (a) hematoxylin–eosin staining; (b) immunohistochemistry for single-strand DNA; (c) TUNEL; (d) TUNEL (green) with propidium iodide (red); magnification: ×400.

Please cite this article in press as: Omokawa, Y., et al., *In vitro* and *in vivo* anti-tumor effects of novel Span 80 vesicles containing immobilized *Eucheuma serra* agglutinin. Int. J. Pharm. (2010), doi:10.1016/j.ijpharm.2010.01.033

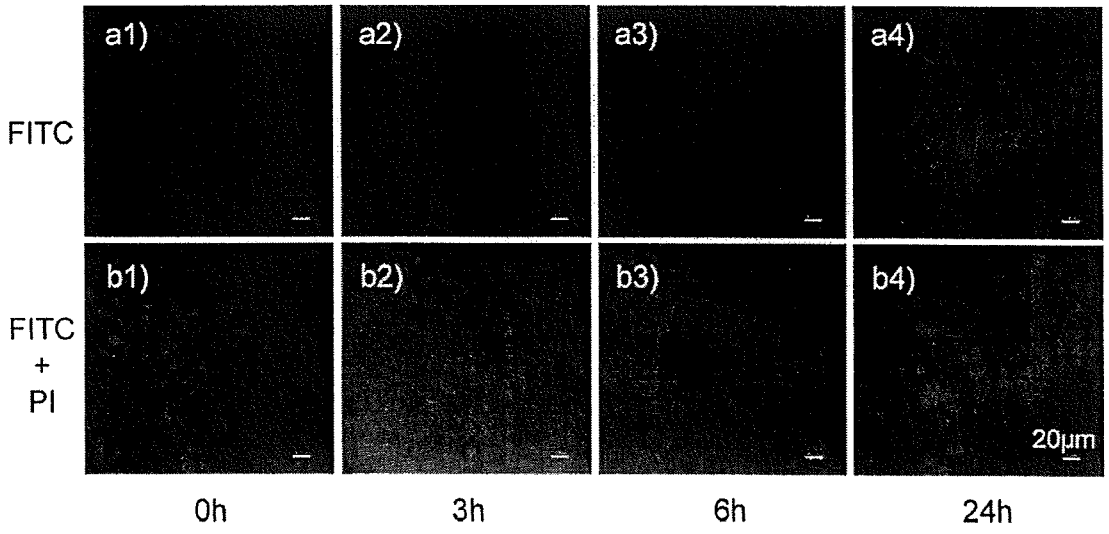

Fig. 9. Accumulation and internalization of **EPV** containing FITC (**FITC-EPV**) into Colon26 tumor cells in tumor-bearing mice. The fluorescence micrographs of the tumors at 0, 3, 6, 24 h after the injection of FITC-EPV with of FITC (green fluorescence) were shown in (a1–a4), respectively. The DNA-stained fluorescence micrographs of the above tumors, also labeled with propidium iodide (red fluorescence), were shown in (b1–b4): the micrographs of b1, b2, b3 and b4 correspond to those of a1, a2, a3, and a4, respectively. Scale bars: 20 μm.

apoptosis in Colo201 tumor grafts after **EPV** administration *in situ* (Fig. 8).

The TUNEL methods revealed numerous apoptotic signals in the tumor tissue, especially at the perivascular area as shown in Fig. 8c and d. Also, immunohistochemistry for ssDNA presented positive signals on the Colo201 tumor cells in mice which were treated with **EPV** (Fig. 8b). These signals were manifested mainly around the intratumoral blood vessels, suggesting that the cell death was induced *via* different mechanisms from that of central necrosis of the tumor which might be mainly induced by anoxia. Thus, these evidences might imply that **EPV** could induce apoptosis of tumor cells around the blood vessels with migration throughout the vessel walls. It seems that **EPV** caused the anti-tumor effect *in vivo* by inducing apoptosis in tumor cells. This is in agreement with the DNA laddering analysis of **EV**-treated cancer cells *in vitro* (Fig. 3d).

3.8. Drug internalization of EPV to tumor cells

For clarifying whether **EPV** could deliver the encapsulated-drug into a tumor *in vivo*, **EPV** containing encapsulated FITC (**FITC-EPV**) were injected intravenously into a Balb/cByjJcl mouse which contained a transplanted Colon26 tumor. The fluorescence micrographs of the mouse tumor were measured *in situ* (Fig. 9). In the tumor, the green fluorescence of **FITC-EPV** gradually increased with time at 6 h and 24 h after the injection, and the presence of FITC in the cytoplasm of tumor cells was confirmed, suggesting that FITC encapsulated in **EPV** was internalized into the cytoplasm of the tumor cells. This indicates that **EPV** could deliver the encapsulated-drug mimics (FITC) into tumor cells.

4. Concluding remarks

The novel lectin *E. serra* agglutinin (ESA) was immobilized onto Span 80 vesicles and the vesicles were investigated with respect to their potential as novel type of nonionic vesicular drug delivery system. The various measurements carried out indicate that the vesicles are rather promising systems for further exploring their usefulness for the delivery of encapsulated anti-tumor drugs. This optimistic conclusion is based on the following: (i) ESA on the surface of Span 80 vesicles showed hemagluttinating activity similar to free ESA, i.e. immobilization onto the vesicles did not lead to an inhibition of the biological activity; (ii) the vesicles showed apoptotic tumor cell cytotoxicity with little effects on the viability of the normal cells tested; (iii) the growth of implanted Colo201 tumors in nude mice could be reduced upon *i.v.* injection of the vesicles; (iv) the presence of fluorescent molecules originally trapped inside the vesicles was enriched in the tumor of tumor-bearing mice at 6 h after *i.v.* administration of the vesicles; (v) with respect to tumor accumulation after 6 h, **EV** and **EPV** are superior as compared to **PV** and **CV**. In the case of the uptake by the RES, **EV**, **PV** and **EPV** are superior as compared to **CV**.

From the study presented, there are two main results. First, the experiments carried out indicate that there is a considerable potential of using Span 80 vesicles as DDS for the treatment of tumor cells, as alternative system to conventional phospholipid-based vesicles. Second, ESA immobilized onto Span 80 vesicles shows anti-tumor activity, especially, if the vesicles contain PEGylated lipids. Span 80 vesicles containing immobilized ESA and PEGylated lipids (**EPV**) are lipidic microcapsules which show *in vivo* anti-tumor activity by themselves, without any entrapped anti-tumor agents. Experiments in which this type of Span 80 vesicles (**EPV**) containing encapsulated anti-tumor drugs is used, are in progress.

Acknowledgements

This study was partly supported by a Grant-in-Aid for the Promotion of Regional Cooperation (No.11793006) and a Grant-in-Aid of Scientific Research for Basic Research (B) (No.10450297) from the Ministry of Education, Culture, Sports, Science and Technology of Japan.

We first thank the graduate students (Ehime University) of Mr. Hideki Takenori, Mr. Yuuki Maruyama, Mr. Souichirou Kuwahara, Mr. Tsuyoshi Nakashita, Mr. Norikazu Yoshimura, Miss Miho Hayashi and Miss Ayako Fukuda for help of the experimental works on this study. The animal experiments in this study were supported by the Department of Molecular Science, Integrated Center for Sciences (INCS) of Ehime University. We are very grateful to Prof. Masato Nose, Prof. Norihiko Tateishi, Dr. Youji Suzuki (Ehime University, School of Medicine, Japan), and Dr. Takashi Fujiwara (Ehime University, INCS, Japan) for the discussion regarding the *in vivo* experiments and to Dr. Norio Koine for helping with the IAOE

Please cite this article in press as: Omokawa, Y., et al., *In vitro* and *in vivo* anti-tumor effects of novel Span 80 vesicles containing immobilized *Eucheuma serra* agglutinin. Int. J. Pharm. (2010), doi:10.1016/j.ijpharm.2010.01.033

synthesis. Also, we thank Mr. Masachika Shudo (Ehime University, INCS, Japan) and Dr. Kazuhiro Akama (NOF corporation, Tokyo, Japan) for their help in the electron microscopy of the vesicles, Mr. Akinori Suginaka of NOF Corporation (Tokyo, Japan) for providing the PEG lipid (Sunbright DSPE-020HCN) and Mr. Gao Lu (McMaster, Canada) for his help with the English and Kikuyo Kato for her help in the organization of the data.

Appendix A. Supplementary data

Supplementary data associated with this article can be found, in the online version, at doi:10.1016/j.ijpharm.2010.01.033.

References

Allen, T.M., 1994. Long-circulating (sterically stabilized) liposomes for targeted drug delivery. Trends Pharmacol. Sci. 15, 215–220.
Allen, T.M., Cullis, P.R., 2004. Drug delivery systems: entering the mainstream. Science 303, 1818–1822.
Barenholz, Y., 2001. Liposome application: problems and prospects. Curr. Opin. Colloid Interface Sci. 6, 66–77.
Couvreur, P., Vauthier, C., 2006. Nanotechnology: intelligent design to treat complex disease. Pharm. Res. 23, 1417–1449.
Ferrari, M., 2005. Cancer nanotechnology: opportunities and challenges. Nat. Rev. Cancer 5, 161–171.
Forssen, E., Willis, M., 1998. Ligand-targeted liposomes. Adv. Drug Deliv. Rev. 29, 249–271.
Foulon, C.F., Reist, C.J., Bigner, D.D., Zalutsky, M.R., 2000. Radioiodination via D-amino acid peptide enhances cellular retention and tumor xenograft targeting of an internalizing anti-epidermal growth factor receptor variant III monoclonal antibody. Cancer Res. 60, 4453–4460.
Fukuda, Y., Sugahara, T., Ueno, M., Fukuta, Y., Ochi, Y., Akiyama, K., Miyazaki, T., Masuda, S., Kawakubo, A., Kato, K., 2006. The anti-tumor effect of *Euchema serra* agglutinin on colon cancer cells *in vitro* and *in vivo*. Anti-Cancer Drugs 17, 943–947.
Gabizon, A., Goren, D., Horowitz, A.T., Tzemach, D., Lossos, A., Siegal, T., 1997. Long-circulating liposomes for drug delivery in cancer therapy: a review of biodistribution studies in tumor-bearing mice. Adv. Drug Deliv. Rev. 24, 337–344.
Garg, A., Tisdale, A.W., Haidari, E., Kokkoli, E., 2009. Targeting colon cancer cells using PEGylated liposomes modified with a fibrionectin-mimetic peptide. Int. J. Pharm. 366, 201–210.
Gortzi, O., Antimisiaris, S.G., Klepetsanis, P., Papadimitriou, E., Ioannou, P.V., 2003. Arsenoliposomes: effect of arsenolipid acyl chain length and vesicle composition on their toxicity towards cancer and normal cells in culture. Eur. J. Pharm. Sci. 18, 175–183.
Hashizume, S., Sato, S., Matsuyama, M., Tamaki, S., Hanada, K., Murakami, H., Yasumoto, K., Nomoto, K., Nakano, K., Kusakabe, K., 1990. Accumulation of ^{125}I-labelled human monoclonal antibody (HB4C5), specific to lung cancer, into transplanted human lung cancer in nude mouse. In: Murakami, H. (Ed.), Trends in Animal Cell Culture Technology, Kodansha. VCH, Tokyo, pp. 167–172.
Hatziantoniou, S., Dimas, K., Georgopoulos, A., Sotiriadou, N., Demetzos, C., 2006. Cytotoxic and anti-tumor activity of liposome-incorporated sclareol against cancer cell lines and human colon cancer xenografts. Pharm. Res. 53, 80–87.
Hori, K., Sato, Y., Ito, K., Fujiwara, Y., Iwamoto, Y., Makino, H., Kawakubo, A., 2007. Strict specificity for high-mannose type *N*-glycans and primary structure of a red alga *Eucheuma serra* lectin. Glycobiology 17, 479–491.
Inoue, K., 1974. Phosphatidylcholine (lecithin). In: Yamakawa, T., Nojima, S. (Eds.), Seikagaku Jikken Kouza, vol. 3. Shishitsu no Kagaku, Tokyo Kagaku Dojin, Tokyo, pp. 257–258.
Ioannou, Y.A., Chen, F.W., 1996. Quantitation of DNA fragmentation in apoptosis. Nucleic Acids Res. 24, 992–993.
Karasaki, Y., Tsukamoto, S., Mizusaki, K., Sugiura, T., Gotoh, S., 2001. A garlic lectin exerted an anti-tumor activity and induced apoptosis in human tumor cells. Food Res. Int. 34, 7–13.
Kato, K., Hirashita, J., 1997. Preparation and function of a hybrid-type vesicle modified by Concanavalin A for a DDS directed toward a cancer therapy. In: Proceeding of the 4th Asia-Pacific Biochemical Engineering Conference (APBioChEC'97), Beijing, 10–23 October 1997, pp. 592–596.
Kato, K., Hirata, K., 1996. Water permeability through the lipid membrane of a giant vesicle prepared by a two-step emulsification technique. Solv. Extr. Res. Dev. Jpn. 3, 62–78.
Kato, K., Ikeda, T., Shinozaki, M., 1993. Lipid membrane characteristic of large lipid vesicles prepared by two-step emulsification technique and enzymatic NAD+-recycling in the vesicles. J. Chem. Eng. Jpn. 26, 212–216.
Kato, K., Walde, P., Mitsui, H., Higashi, N., 2003. Enzymatic activity and stability of D-fructose dehydrogenase and sarcosine dehydrogenase immobilized onto giant vesicles. Biotechnol. Bioeng. 84 (4), 415–423.
Kato, K., Walde, P., Koine, N., Imai, Y., Akiyama, K., Sugahara, T., 2006. Molecular composition of nonionic vesicles prepared from span 80 or span 85 by a two-step emulsification method. J. Dispersion Sci. Technol. 27, 1217–1222.
Kato, K., Walde, P., Koine, N., Ichikawa, S., Nagahama, T.R., Ishihara, T., Tsujii, T., Shudou, M., Omokawa, Y., Kuroiwa, T., 2008. Temperature-sensitive nonionic vesicles prepared from Span 80 (sorbitan monooleate). Langmuir 24, 10762–10770.
Kawakubo, A., Makino, H., Ohnishi, J., Hirohara, H., Hori, K., 1997. The marine red alga *Eucheuma serra* J. Agardh, a high yielding source of two Isolectins. J. Appl. Phycol. 9, 331–338.
Koning, G.A., Kamps, J.A.A.M., Scherphof, G.L., 2002. Efficient intracellular delivery of 5-fluorodeoxyuridine into colon cancer cells by targeted immunoliposomes. Cancer Detect. Prev. 26, 299–307.
Konopka, K., Pretzer, E., Felgner, P.L., Düzgüneş, N., 1996. Human immunodeficiency virus type-1 (HIV-1) infection increases the sensitivity of macrophages and THP-1 cells to cytotoxicity by cationic liposomes. Biochim. Biophys. Acta – Mol. Cell Res. 1312, 186–196.
Korde, A., Venkatesh, M., Sarma, H.D., Pillai, M.R.A., 2000. Preparation and pharmacokinetic evaluation of iodine-125 labeled alphamethyl-L-tyrosine. J. Radioanal. Nucl. Chem. 246, 173–178.
Kuan, C.T., Reist, C.J., Foulon, C.F., Lorimer, I.A.J., Archer, G., Pegram, C.N., Pastan, I., Zalutsky, M.R., Bigner, D.D., 1999. ^{125}I-labeled anti-epidermal growth factor receptor-vIII single-chain Fv exhibits specific and high-level targeting of glioma xenografts. Clin. Cancer Res. 5, 1539–1549.
Larsson, J., Wingardh, K., Berggard, T., Davies, J.R., Logdberg, L., Strand, S.E., Akerstrom, B., 2001. Distribution of iodine 125-labeled α1-microglobulin in rats after intravenous injection. J. Lab. Clin. Med. 137, 165–175.
Lian, T., Ho, R.J.Y., 2001. Trends and developments in liposome drug delivery systems. J. Pharm. Sci. 90, 667–680.
Lowry, O.H., Rosebrough, N.J., Farr, A.L., Randall, R.J., 1951. Protein measurement with the Folin phenol reagent. J. Biol. Chem. 193, 265–275.
Martin, S.J., Reutelingsperger, C.P.M., McGahon, A.J., Rader, J.A., Van Schie, R.C.A.A., LaFace, D.M., Green, D.R., 1995. Early redistribution of plasma membrane phosphatidylserine is a general feature of apoptosis regardless of the initiating stimulus: Inhibition by over expression of Bcl-2 and Abl. J. Exp. Med. 182, 1545–1556.
Maruyama, K., Takizawa, T., Takahashi, N., Tagawab, T., Nagaikeb, K., Iwatsuru, M., 1997. Targeting efficiency of PEG-immunoliposome-conjugated antibodies terminals. Adv. Drug Deliv. Rev. 24, 235–242.
Ohama, Y., Heike, Y., Sugahara, T., Sakata, K., Yoshimura, N., Hisaeda, Y., Hosokawa, M., Takashima, S., Kato, K., 2005. Gene transfection into HeLa Cells by vesicles containing cationic peptide lipid. Biosci. Biotechnol. Biochem. 69, 1453–1458.
Peer, D., Karp, J.M., Hong, S., Farokhzad, O.C., Margalit, R., Langer, R., 2007. Nanocarriers as an emerging platform for cancer therapy. Nat. Nanotechnol. 2, 751–760.
Rad, F.H., Le Buanec, H., Paturance, S., Larcier, P., Genne, P., Ryffel, B., Bensussan, A., Bizzini, B., Gallo, R.C., Zagury, D., Uzan, G., 2007. VEGF kinoid vaccine, a therapeutic approach against tumor angiogenesis and metastases. Proc. Natl. Acad. Sci. U.S.A. 104, 2837–2842.
Sato, T., Sunamoto, J., Ishii, N., Koji, K., 1988. Polysaccharide-coated immunoliposomes bearing anti-CEA Fab' fragment and their internalization by CEA-producing tumor cells. J. Bioact. Compat. Polym. 3, 195–204.
Sharma, A., Sharma, U.S., 1997. Liposomes in drug delivery: progress and limitations. Int. J. Pharm. 154, 123–140.
Shirai, T., Watanabe, Y., Lee, M., Ogawa, T., Muramoto, K., 2009. Structure of Rhamnose-binding Lectin CSL3: unique pseudo-tetrameric architecture of a pattern recognition protein. J. Mol. Biol. 391, 390–403.
Sugahara, T., Ohama, Y., Fukuda, A., Hayashi, M., Kawakubo, A., Kato, K., 2001. The cytotoxic effect of *Eucheuma serra* agglutinin (ESA) on cancer cells and its application to molecular probe for drug delivery system using lipid vesicles. Cytotechnology 36, 93–99.
Sugahara, T., Kawashima, S., Oda, A., Hisaeda, Y., Kato, K., 2005. Preparation of cationic immunovesicles containing cationic peptide lipid for specific drug delivery to target cells. Cytotechnology 47, 51–57.
Timoshenko, A.V., Lan, Y., Gabius, H.J., Lala, P.K., 2001. Immunotherapy of C3H/HeJ mammary adenocarcinoma with interleukin-2, mistletoe lectin or their combination: effects on tumor growth, capillary leakage and nitric oxide (NO) production. Eur. J. Cancer 37, 1910–1920.
Torchilin, V.P., 2005. Recent advances with liposomes as pharmaceutical carriers. Nat. Rev. Drug Discov. 4, 145–160.
Wang, H., Gao, J., Ng, T.B., 2000. A new lectin with highly potent antihepatoma and antisarcoma activities from the oyster mushroom *Pleurotus ostreatus*. Biochem. Biophys. Res. Commun. 275, 810–816.
Zeisig, R., Shimada, K., Hirota, S., Arndt, D., 1996. Effect of sterical stabilization on macrophage uptake *in vitro* and on thickness of the fixed aqueous layer of liposomes made from alkylphosphocholines. Biochim. Biophys. Acta 1285, 237–245.

Please cite this article in press as: Omokawa, Y., et al., *In vitro* and *in vivo* anti-tumor effects of novel Span 80 vesicles containing immobilized *Eucheuma serra* agglutinin. Int. J. Pharm. (2010), doi:10.1016/j.ijpharm.2010.01.033

doi: 10.1111/j.1365-2222.2009.03229.x

Clinical & Experimental Allergy, 39, 972–981

ORIGINAL ARTICLE **Asthma and Rhinitis**

Gene-expression profiles in human nasal polyp tissues and identification of genetic susceptibility in aspirin-intolerant asthma

T. Sekigawa*,†, A. Tajima*, T. Hasegawa†, Y. Hasegawa‡, H. Inoue§, Y. Sano¶, S. Matsune‖, Y. Kurono‖ and I. Inoue*,**

**Department of Molecular Life Science, Tokai University School of Medicine, Isehara, Japan, †Division of Respiratory Medicine, Niigata University Graduate School of Medical and Dental Sciences, Niigata, Japan, ‡Department of Internal Medicine, Nagoya University School of Medicine, Nagoya, Japan, §Research Institute for Diseases of the Chest, Kyushu University Faculty of Medicine, Fukuoka, Japan, ¶Doai Memorial Hospital, Tokyo, Japan, ‖Department of Otolaryngology, Head and Neck Surgery, Kagoshima University Graduate School of Medical and Dental Sciences, Kagoshima, Japan and **Core Research for Evolutional Science and Technology, Japan Science and Technology Corporation, Kawaguchi, Japan*

Clinical & Experimental Allergy

Correspondence:
Atsushi Tajima, Department of Molecular Life Science, Tokai University School of Medicine, 143 Shimokasuya, Isehara, Kanagawa 259-1193, Japan.
E-mail: atajima@is.icc.u-tokai.ac.jp
Cite this as: T. Sekigawa, A. Tajima, T. Hasegawa, Y. Hasegawa, H. Inoue, Y. Sano, S. Matsune, Y. Kurono and I. Inoue, *Clinical & Experimental Allergy*, 2009 (39) 972–981.

Summary

Background Aspirin-intolerant asthma (AIA) is a subtype of asthma induced by non-steroidal anti-inflammatory drugs and characterized by an aggressive mucosal inflammation of the lower airway (asthma) and the upper airways (rhinitis and nasal polyp). The lower airway lesion and the nasal polyp in AIA are postulated to have common pathogenic features involving aspirin sensitivity that would be reflected in the gene expression profile of AIA polyps.

Objective This study was conducted to clarify the pathogenesis of AIA using gene expression analysis in nasal polyps, and identify genetic susceptibilities underlying AIA in a case–control association study.

Methods Global gene expression of nasal polyps from nine AIA patients was examined using microarray technology in comparison with nasal polyps from five eosinophilic sinusitis (ES) patients, a related disease lacking aspirin sensitivity. Based on the AIA-specific gene expression profile of nasal polyp, candidate genes for AIA susceptibility were selected and screened by a case–control design of 219 AIA patients, 374 non-asthmatic control (CTR), and 282 aspirin-tolerant asthmatic (ATA) subjects.

Results One hundred and forty-three elevated and three decreased genes were identified as AIA-specific genes that were enriched in immune response according to Gene Ontology analysis. In addition, a *k*-means-based algorithm was applied to cluster the genes, and a subclass characteristic of AIA comprising 18 genes that were also enriched in immune response was identified. By examining the allelic associations of single nucleotide polymorphisms (SNPs) of AIA candidate genes relevant to an immune response with AIA, two SNPs, one each of *INDO* and *IL1R2*, showed significant associations with AIA ($P = 0.011$ and 0.026 after Bonferroni's correction, respectively, in AIA vs. CTR). In AIA–ATA association analysis, modest associations of the two SNPs with AIA were observed.

Conclusion These results indicate that *INDO* and *IL1R2*, which were identified from gene expression analyses of nasal polyps in AIA, represent susceptibility genes for AIA.

Keywords aspirin-intolerant asthma, candidate genes, genetic association, genome-wide gene expression, single nucleotide polymorphism

Submitted 5 March 2008; revised 11 January 2009; accepted 26 January 2009

Introduction

In some asthmatic patients, aspirin and several other non-steroidal anti-inflammatory drugs (NSAIDs) that inhibit cyclooxygenase enzymes (COXs) induce a severe asthmatic attack, a disease known as aspirin-intolerant asthma (AIA) [1, 2]. Several large surveys have concluded that the incidence of AIA in adult asthmatic patients is 5–15% based on patients' histories alone, but the frequency becomes two to three times higher when adult asthmatic

patients are challenged with aspirin. In women, AIA is overrepresented in a ratio of 2.3 : 1 and is more severe and has an earlier onset. AIA patients have typical clinical features including asthma, aspirin sensitivity, and bilateral nasal polyps, known as Samter's triad. Despite the well-defined pharmacological trigger, the molecular pathogenesis of AIA is still unclear. The usual hypothesis is a disturbance in the metabolism of arachidonic acid, because aspirin and NSAIDs target COXs, key enzymes of the prostaglandin biosynthetic pathway. However, the precise pathogenesis requires further investigation.

There is a moderate genetic background in AIA: the European Network on Aspirin-Induced Asthma found that 5.8% of 500 AIA patients had a family history of aspirin sensitivity [3]. First, a polymorphism in the promoter of leukotriene C_4 synthase, A-444C, was reported to be associated with AIA in Polish patients [4, 5]. A recent report showed that a haplotype of the 5-lipoxygenase gene was weakly associated with AIA in a Korean population [6]. With an extensive candidate gene analysis related to arachidonic acid metabolism, our group reported that single nucleotide polymorphisms (SNPs) in the prostaglandin E_2 receptor subtype 2 gene were significantly associated with AIA, and the functional impact of a promoter variant was further demonstrated [7]. Most recently, SNPs in prostaglandin E_2 receptor subtype 3 gene were associated in Korean population [8].

In the past few years, microarray techniques for gene expression profiling have been applied to a wide range of biological problems and have contributed to the discoveries of complex networks of biochemical processes underlying complex diseases. Microarray techniques have also helped to identify novel biomarkers, disease subtypes, and discrepancies of gene expression in human populations. Despite the advances in microarray techniques, application of the technology to identify susceptibility genes underlying complex diseases appears to be unsuccessful so far, with some exceptions [9, 10].

AIA is characterized by an aggressive mucosal inflammation of the lower airway (asthma) and the upper airways (rhinitis and nasal polyp). Rhinitis symptoms first occur in most AIA patients before the development of asthmatic intolerance to aspirin and other NSAIDs, whereas nasal polyps in AIA patients are first diagnosed at almost the same time aspirin intolerance appears [3]. We postulated that the lower airway lesion and the polyp in AIA have a common pathophysiology of aspirin intolerance, suggesting the nasal polyp as a pleiotropic genetic model of the bronchial inflammation of AIA. Global gene expression of the nasal polyps of AIA patients was examined using microarray technology for comparison with nasal polyps of eosinophilic sinusitis (ES) patients: ES is typically characterized by a nasal polyp with an inflammatory cell infiltration similar to that in an AIA polyp but without aspirin sensitivity, thus being an appropriate reference for the selection of AIA-specific genes.

Materials and methods

Nasal polyp tissues and Aspirin-Intolerant Asthma Subjects

Nasal polyp tissues for microarray analysis were obtained from nine Japanese patients (aged from 35 to 76 years, five males/four females) with AIA, five (aged from 34 to 73 years, three males/two females) with ES, and two (aged 61 and 71 years, both males) with only chronic sinusitis (CS) (Table 1). These patients had not been exposed to preoperative treatment with steroids for at least 1 year before surgery. According to the definition of rhinosinusitis, CS with nasal polyps with eosinophilic inflammatory features without fungal hyphae includes aspirin-sensitive and aspirin-tolerant types [11]. Thus, three groups of patients with nasal polyps were sequentially defined as follows: first, CS with nasal polyps was diagnosed based on clinical symptoms, such as nasal discharge, postnasal drip, headache, hyposmia, and nasal obstruction, and endonasal findings of muco-purulent secretion and nasal polyps with a paranasal shadow observed by CT examination [12]. Among CS patients with nasal polyps, ES patients were identified histologically by counting the number of eosinophils at ×200 magnification under light microscopy. Five fields were examined for each section,

Table 1. Clinical characteristics of patients with nasal polyps for microarray analysis

ID	Age/ gender	Parameters in peripheral blood		Allergic rhinitis	Asthma	AIA episode
		WBC (/mm^3)	Eosinophil (%)			
AIA#1	76/M	8000	3	−	+	+
AIA#2	48/M	5500	13	−	+	+
AIA#3	73/M	6500	3	−	+	+
AIA#4	59/F	9500	28	−	+	+
AIA#5	50/F	5720	14	−	+	+
AIA#6	40/M	9100	4	−	+	+
AIA#7	35/M	8800	6	−	+	+
AIA#8	50/F	6000	9	+	+	+
AIA#9	66/F	7000	8	−	+	+
ES#1	73/F	7200	2	−	+	−
ES#2	64/F	6400	23	−	+	−
ES#3	69/M	7700	4	+	−	−
ES#4	61/M	4900	5	−	+	−
ES#5	34/M	6300	3	+	+	−
CS#1	61/M	7400	10	−	+	−
CS#2	67/M	9700	10	−	−	−

M, male; F, female; WBC, white blood cell; −, no allergic rhinitis, no asthma, or no AIA episode; AIA, aspirin-intolerant asthma; CS, chronic sinusitis; ES, eosinophilic sinusitis.

and the average was considered to be the number of eosinophils infiltrating the sample. Nasal polyps having more than 100 eosinophils were classified as ES [12]. Among ES patients, those who had had apparent episodes of asthma attacks in response to aspirin and other NSAIDs were classified as AIA patients (AIA#1–9). The remaining five ES patients without AIA episodes (ES#1–5) had no troubles even after taking NSAIDs in postoperative courses during hospitalization. The oral provocation test for AIA patients was not performed in most of the patients due to potential risk, although severe reactions against the provocation were improbable [13], and only verbal history has yielded some false positives [14]. The ethics committees of Kagoshima University approved the study protocols, and each participant gave written informed consent.

DNA samples from 219 unrelated individuals with AIA (age: 55.7±13.5 years; 70 males/149 females) and 374 non-asthmatic controls (CTR) (age: 44.5±23.2 years; 181 males/193 females) were obtained as described previously [7]. For AIA-associated SNPs, 282 unrelated individuals with aspirin-tolerant asthma (ATA) (age: 56.0±16.1 years; 132 males/150 females) [7] were also genotyped, and used as asthmatic controls. The subjects were recruited at Niigata University Hospital, University of Tokyo Hospital, Nagoya University Hospital, Doai Memorial Hospital, and Kyushu University Hospital, with Institutional Review Board approvals. The diagnosis of AIA was based on a self-reported history due to the potential risk of a provocation test. ATA was defined as adult asthma diagnosed by expert physicians according to the American Thoracic Society criteria [15] and no history of aspirin or NSAID-induced asthmatic attack, and comprised of 154 atopic asthmatic (age: 48.0±15.6 years; 80 male/74 female) and 128 non-atopic asthmatic (age: 65.9±10.0 years; 52 male/76 female) subjects. CTR were outpatients with diseases (e.g., hypertension) other than respiratory diseases including asthma, and who self-reported no history of aspirin sensitivity. The patients and controls were all of Japanese ethnicity. Although the Japanese population is thought to be genetically homogenous, nearly identical numbers of patients and controls from the various locations were recruited to avoid geographical differences in allelic frequencies.

RNA extraction

The nasal polyp tissue was removed during endoscopic sinus surgery, submerged in RNA*later* regent (Ambion Inc., Austin, TX, USA) to avoid RNA degradation, and used for RNA extraction within 48 h after resection. Total RNA was extracted using TRIzol reagent (Invitrogen, Carlsbad, CA, USA) according to the manufacturer's instructions. The quality and quantity of the extracted RNA were analysed using the Agilent 2100 bioanalyzer (Agilent Technologies Inc., Palo Alto, CA, USA) with an RNA6000 Nano LabChip Kit (Agilent Technologies). RNAs from two CS patients were equally pooled, and used as a common reference in the two-colour microarray experiments, where a single microarray was used to compare each test sample from an AIA or an ES patient with the reference sample.

cRNA synthesis, labelling, hybridization, and expression profiling

For fluorescent cRNA synthesis, high-quality total RNA (150 ng) was labelled with the Low RNA Input Fluorescent Linear Amplification Kit (Agilent Technologies) according to the manufacturer's instructions. In this procedure, cyanine 5-CTP (Cy5) and cyanine 3-CTP (Cy3) (PerkinElmer, Boston, MA, USA) were used to generate labelled cRNA from the individual AIA or ES RNA and the pooled CS RNA as a reference, respectively. Labelled cRNAs (0.75 μg each) from the AIA, ES, or CS patients were fragmented in a hybridization mixture with the In Situ Hybridization Kit Plus (Agilent Technologies) according to the manufacturer's instructions. The mixture was hybridized for 17 h at 65 °C to an Agilent Human 1A(v2) Oligo Microarray. After hybridization, the microarray was washed with SSC buffer, and then scanned in Cy3 and Cy5 channels with the Agilent DNA Microarray Scanner, model G2565AA. Signal intensity per spot was generated from the scanned image with Feature Extraction Software ver7.5 (Agilent Technologies) in default settings. Spots that did not pass quality control procedures with the software were flagged and removed for further analysis.

GeneSpring software GX 7.3 (Agilent Technologies) was used for the Lowess (locally weighted linear regression curve fit) normalization of the ratio (Cy5/Cy3) of the signal intensities generated in each microarray and the subsequent data analysis. To determine the AIA-specific expression profile of nasal polyps, ES transcripts with ratios ranging from 0.5 to 2 were extracted, and the AIA transcripts with expression undergoing a twofold change or more were extracted as decreased or elevated genes. Of the transcripts overlapping the two groups, only those with statistically significant differences in expression between the AIA and CS nasal polyps (Benjamini and Hochberg false discovery rate (FDR)<0.01; [16]) were counted as AIA-specific genes. To identify novel expression patterns in nasal polyps from AIA patients, the *k*-means method [17], a well-known unsupervised partitional clustering approach, was applied to the AIA-specific genes. For functional subclassification of the AIA-specific genes, we applied the Gene Ontology (GO) classification for biological processes with DAVID 2.1 (http://david.abcc.ncifcrf.gov/), a web-accessible program [18]. A permutation test with 10 000 iterations was used for multiple test correction when nasal polyps from AIA

and ES patients were compared at the transcriptome level [19]. $P<0.05$ was considered significant in every statistical analysis.

Quantitative real-time reverse transcription polymerase chain reaction analysis

Two transcripts, *INDO* and *IL1R2*, that were differentially expressed between AIA and CS nasal polyps were subjected to real-time reverse transcription polymerase chain reaction (RT-PCR) for verification of the microarray data, using a validation set of total RNAs from AIA ($n = 10$) and CS ($n = 4$) nasal polyps including nine AIA and two CS samples for the present microarray experiment. Total RNA from each nasal polyp was used as a template in first-strand cDNA synthesis with the SuperScript III First-Strand Synthesis System (Invitrogen). Real-time PCR was performed using TaqMan Gene Expression Assays (Applied Biosystems, Tokyo, Japan) with TaqMan Universal PCR Master Mix (Applied Biosystems) on an ABI PRISM 7900HT Sequence Detection System (Applied Biosystems) according to the manufacturer's instructions. The relative quantification method [20] was used to measure the amounts of the respective genes in nasal polyps, normalized to *GAPDH* as an endogenous control. The statistical significance in gene expression between the AIA and the CS samples was determined by the Welch t-test; $P<0.05$ was considered significant.

Single nucleotide polymorphism genotyping

For gene-based association analysis, SNPs of AIA candidate genes were obtained from the NCBI dbSNP database (http://www.ncbi.nlm.nih.gov/SNP/) using SNPbrowser Software (Applied Biosystems), to cover the entire regions of the genes positionally and genetically. SNPs were genotyped using the TaqMan SNP Genotyping assay (Applied Biosystems) with the allelic discrimination software SDS version 2.1 (Applied Biosystems) on the ABI PRISM 7900HT Sequence Detection System (Applied Biosystems) according to the manufacturer's instructions.

Statistical analysis of association study

Differences in allelic frequencies were evaluated by a case–control design with a χ^2 test. Haplotype frequencies for multiple loci were estimated using the expectation-maximization method with SNPAlyze v6.0 software (DYNACOM, Mobara, Japan). Bonferroni's correction was adopted for each gene and haplotype for multiple test correction.

Pairwise LD was estimated as $D = x_{11} - p_1 q_1$ where x_{11} is the frequency of haplotype A_1B_1, and p_1 and q_1 are the frequencies of alleles A1 and B1 at loci A and B, respectively. A standardized LD coefficient, r, is given by $D/(p_1 p_2 q_1 q_2)^{1/2}$, where p_2 and q_2 are the frequencies of the other alleles at loci A and B, respectively [21]. Lewontin's coefficient, D', is given by $D' = D/D_{max}$, where $D_{max} = \min(p_1 q_2, p_2 q_1)$ when $D > 0$ or $D_{max} = \min(p_1 q_1, p_2 q_2)$ when $D < 0$ [22].

The power of the present association analysis was calculated using 'Genetic Power Calculator [23] (http://pngu.mgh.harvard.edu/~purcell/gpc/)'. Using our sample sizes in the AIA–CTR comparison, the study has had 80% power to detect common alleles (risk allele frequency = 0.1) with a relative risk of 1.65, and 50% power to detect the alleles with a relative risk of 1.44 at a threshold of nominal P-value = 0.05 under an additive model in the log-odds scale.

Results and discussion

Microarray analysis of nasal polyp tissues of Aspirin-Intolerant Asthma patients

Bronchial biopsy specimens from AIA patients exhibit a fourfold increase in eosinophils compared with those from ATA patients [24]. The increased influx of eosinophils into the airway mucosa of AIA patients is likely a result of an inflammatory rather than an atopic mechanism. It is noteworthy that the nasal polyps of AIA patients show very similar pathological characteristics such as infiltration of eosinophils into the bronchial mucosa [12, 13]. These observations led us to postulate a common molecular mechanism in the development of a polyp and AIA. In such a case, genes related to nasal polyp development in AIA patients might suggest both potential susceptibility genes and pathways involved in aspirin hypersensitivity and the development of AIA. Because it is not practical to apply bronchial tissues for microarray analysis, we used nasal polyp tissues from AIA patients that were under resection for therapeutic purpose and monitored global gene expressions to demonstrate AIA-specific gene expression profiles. ES is known to be a related disorder of AIA; ES is typically characterized by a nasal polyp with inflammatory cell infiltration similar to that in an AIA polyp but without aspirin sensitivity, thus being an appropriate reference for the selection of AIA-specific genes.

The global gene expression profiles of AIA nasal polyps and those of ES nasal polyps were then compared. Similar expression profiles were expected in polyps of AIA and ES patients due to the similar histological and biochemical characteristics such as extensive infiltration of eosinophils. Figure 1a shows a hierarchical clustering (HC) dendrogram for the profiles of nasal polyps from nine AIA and five ES patients. Unexpectedly, two discrete clusters appeared, representing AIA and ES nasal polyps, respectively, with the exception of one (ES#5) of the ES tissues, from a patient who was aspirin tolerant and had clinical characteristics similar to those of other ES patients

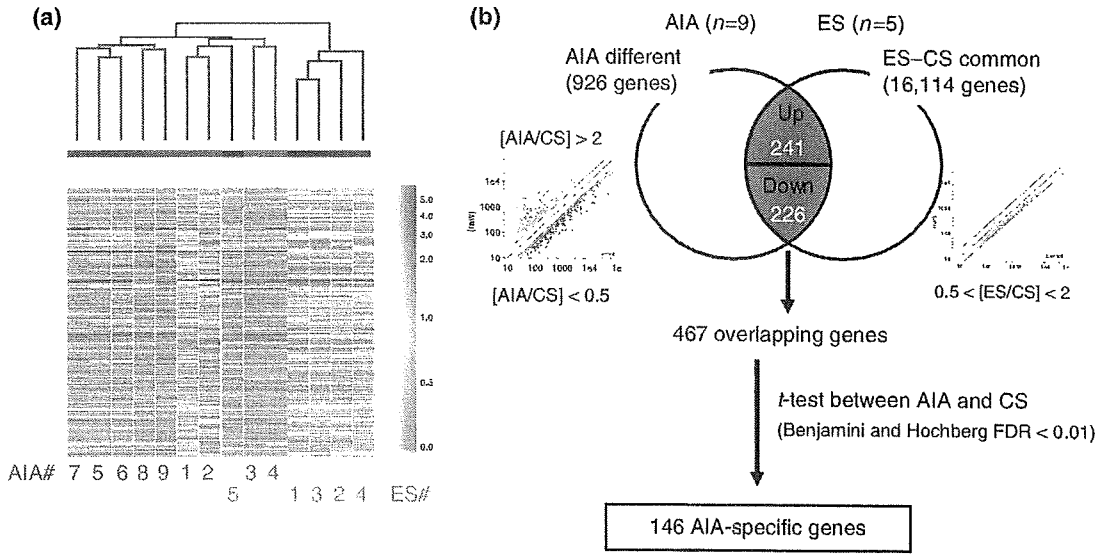

Fig. 1. Experimental design to extract aspirin-intolerant asthma (AIA)-specific genes with microarray analysis. (a) Hierarchical clustering (HC)-based classification of nasal polyps from AIA and eosinophilic sinusitis (ES) patients. Based on the gene expression in nasal polyps, HC clustering shows distinct expression profiles in AIA and ES patients. The clinical characteristics of the patients for the expression analysis are summarized in Table 1. (b) Strategy for discovering AIA-specific gene expression profiles, referred to as 'AIA-specific genes'. From 16,114 genes representing no change (less than twofold) in gene expression between ES and chronic sinusitis (CS) polyps, 146 AIA candidate genes were extracted at the threshold of twofold differences in expression with statistical significance (FDR < 0.01) between AIA and CS polyps.

(Table 1). Thus, AIA and ES nasal polyps appear to exhibit distinct expression profiles. The HC analysis was supported statistically in that 4012 of 18716 transcripts surveyed by microarray displayed significant differences in expression between the AIA and the ES polyps using a permutation test, followed by Student's *t*-test at a significance level of 0.05. While the expression differences between the two groups could be due to an inter-group variation in cell composition within the nasal polyp tissues, they could not have been due to aspirin sensitivity, and so a two-step selection process was used to extract an AIA-specific expression profile (Fig. 1b). We first obtained genes (16114 genes) common to polyp formation, i.e., genes showing no difference (less than twofold) between ES and chronic sinusitis (CS) polyps, in which a difference in the pathological state of the polyps such as infiltration of inflammatory cells would be minimized. We then selected 926 genes differentially expressed between AIA and CS polyps showing twofold differences, which could be related to the pathophysiology of aspirin sensitivity. From the overlapping genes (467 genes) between the two gene lists, 146 genes were statistically extracted including 143 elevated and three decreased transcripts that were defined as AIA-specific genes.

To examine the biological features of these AIA-specific genes, we assigned 146 genes to the GO classification using the web-accessible DAVID program. As shown in Table 2, nine GO terms were highly associated with the AIA-specific genes. It is notable that the genes involved in cell proliferation and immune response were enriched in the AIA candidate genes, indicating successful extraction of the genes related to nasal polyp formation, because both nasal cell growth and acute inflammation in the respiratory tract are clinical characteristics during the development of nasal polyp in AIA patients.

We then applied the *k*-means algorithm [17], an unsupervised partitional clustering approach, to organize AIA-specific genes into functionally meaningful groups. The *k*-means method has been efficient in showing a significant enrichment of genes belonging to given functional categories in the *k*-means-based clusters [25]. In this analysis, we selected an optimal number of clusters (*k*) in which the number of unclassified genes was minimized. As shown in Table 2, four distinct clusters, subsets 1, 2, 3, and 4, in gene expression were generated for the AIA-specific genes using the *k*-means method (figure not shown). Thus, four types of distinct expression patterns across samples were observed using the dataset of 146 AIA-specific genes. The three genes with decreased expression in AIA nasal polyps were categorized into subset 4, and the 143 elevated genes were classified into three subsets, 1, 2, and 3 (Table 2). Interestingly, genes involved in immune response (18/21 genes) and response to external signal (11/15 genes) were highly enriched in subset 2, while another enrichment of cell proliferation-related genes (17/24 genes) was observed in subset 1 (Table 2). These features of the gene enrichments indicate the biological significance of the present *k*-means-based clusters for AIA candidate genes. According to the cluster–GO correlation, the most notable functional patterning occurred for genes relevant to an immune response owing to the highest concentration (85.7% of the genes

Table 2. Enrichements of genes involved in GO-functional categories within *k*-means-based clusters

GO TERM (biological process; level 3)	Count	*P*-value	*k*-means clusters (no. of genes assigned) Subset 1 ($n = 57$)	Subset 2 ($n = 57$)	Subset 3 ($n = 29$)	Subset 4 ($n = 3$)
Cell proliferation	24	0.0000028	17	7		
Immune response	21	0.068		18	3	
Biopolymer metabolism	20	0.034	9	7	3	
Response to stress	17	0.00097	4	11	2	
Response to external stimulus	15	0.083		11	4	
Catabolism	14	0.017	5	5	4	
Cell organization and biogenesis	12	0.031	2	8		1
Cell motility	6	0.012	2	4		
Cellular defense response	4	0.024		3	1	

DAVID v2.1 (http://david.abcc.ncifcrf.gov/) was used to classify 146 AIA-specific genes functionally according to Gene ontology (GO) classification for biological process. Genes in the respective GO categories were mapped to four *k*-means-based clusters for gene expression.

extracted) in one subset (subset 2) of clusters, indicating that their expression might be highly coordinated in nasal polyps.

Association study with candidate genes for AIA

Based on functional clustering of the AIA-specific genes in the *k*-means clustering, immune response-related genes might serve as candidate genes for susceptibility underlying AIA because the AIA-specific changes in gene expression reflect elevated immune and inflammatory reactions in the nasal polyps of AIA patients. Table 3 shows 21 immune response-related genes in descending order based on the expression ratios in the microarray analysis. We focused on the three top-ranked genes, *INDO*, *IL1R2*, and *CLECSF6*, and screened 17 SNPs of these three genes (three SNPs for *INDO*, 11 SNPs for *IL1R2*, and three SNPs for *CLECSF6*) for an allelic association study between 219 AIA patients and 178 non-asthmatic controls (CTR) in the first screening. One SNP of *INDO* and four SNPs of *IL1R2* were significantly associated with AIA evaluated by a simple χ^2 test (data not shown) based on nominal *P*-values. Differential expressions of the two genes, *INDO* and *IL1R2*, in AIA nasal polyps were confirmed by real-time RT-PCR (Fig. 2). Because the three SNPs of *CLECSF6* examined were not associated with AIA, the gene was not pursued, and other ranked genes were also not screened further.

After increasing the sample size of CTR to 374 subjects, we further examined the allelic associations of a total of 14 SNPs (three SNPs for *INDO* and 11 SNPs for *IL1R2*) with AIA in a second screening. As shown in Tables 4 and 5, one SNP of *INDO* (INDO-SNP2: rs7820268) and one SNP of *IL1R2* (IL1R2-SNP10: rs11688145) showed significant associations with AIA after a multiple test correction using Bonferroni's correction (corrected $P = 0.011$ for the INDO-SNP2 and corrected $P = 0.026$ for the IL1R2-SNP10). None of the SNPs in the controls showed deviation from Hardy–Weinberg's equilibrium (data not shown). Both the significant SNPs observed were located in non-coding regions of the respective genes, and so the functional impacts of the SNPs were not demonstrated. In order to examine whether *INDO* and *IL1R2* were genetic

Table 3. Twenty-one genes involved in *immune response*

	Expression ratio (normalized)	Gene Symbol	Name
1	3.70	INDO	Indoleamine-pyrrole 2,3 dioxygenase
2	3.31	IL1R2	Interleukin 1 receptor, type II
3	2.75	CLECSF6	C-type lectin, superfamily member 6
4	2.68	CCL11	Chemokine (C-C motif) ligand 11
5	2.65	CD163	CD163 antigen
6	2.63	TNFSF10	Tumour necrosis factor (ligand) superfamily, member 10
7	2.53	AIF1	Allograft inflammatory factor 1
8	2.46	NCF2	Neutrophil cytosolic factor 2
9	2.32	ALOX5AP	Arachidonate 5-lipoxygenase-activating protein
10	2.31	FPR1	Formyl peptide receptor 1
11	2.21	TYROBP	TYRO protein tyrosine kinase-binding protein
12	2.21	CTSC	Cathepsin C
13	2.11	IFI30	Interferon, gamma-inducible protein 30
14	2.03	MICB	MHC class I polypeptide-related sequence B
15	1.90	LCP2	Lymphocyte cytosolic protein 2
16	1.86	NCK1	NCK adaptor protein 1
17	1.84	LST1	Leukocyte-specific transcript 1
18	1.83	TLR2	Toll-like receptor 2
19	1.76	PTAFR	Platelet-activating factor receptor
20	1.71	CKLF	Chemokine-like factor
21	1.65	EDG6	Endothelial differentiation, G-protein-coupled receptor 6

